NASA TECHNICAL NOTE

NASA TN D-4116

NASA TN D-4116

EFFECTS OF A SIMULATED SPACE ENVIRONMENT ON THERMAL RADIATION CHARACTERISTICS OF SELECTED BLACK COATINGS

by William R. Wade and Donald J. Progar

Langley Research Center
Langley Station, Hampton, Va.

NATIONAL AERONAUTICS AND SPACE ADMINISTRATION • WASHINGTON, D. C. • SEPTEMBER 1967

ERRATA

NASA Technical Note D-4116

EFFECTS OF A SIMULATED SPACE ENVIRONMENT ON THERMAL RADIATION CHARACTERISTICS OF SELECTED BLACK COATINGS

By William R. Wade and Donald J. Progar

September 1967

Page 3, sixth line from bottom: The current density should be 0.01725 amp/cm^2 instead of 0.1725 amp/cm^2.

Issued 10-24-68

NASA TN D-4116

EFFECTS OF A SIMULATED SPACE ENVIRONMENT ON THERMAL RADIATION CHARACTERISTICS OF SELECTED BLACK COATINGS

By William R. Wade and Donald J. Progar

Langley Research Center
Langley Station, Hampton, Va.

NATIONAL AERONAUTICS AND SPACE ADMINISTRATION

For sale by the Clearinghouse for Federal Scientific and Technical Information
Springfield, Virginia 22151 – CFSTI price $3.00

EFFECTS OF A SIMULATED SPACE ENVIRONMENT ON THERMAL RADIATION CHARACTERISTICS OF SELECTED BLACK COATINGS

By William R. Wade and Donald J. Progar
Langley Research Center

SUMMARY

Black coatings were prepared by various processes for possible use as stable, highly absorbing surfaces for spacecraft or as flat absorbers for use in ground-test space-simulation facilities in the wavelength range from 0.25 μm to 25.0 μm.

The coatings were subjected to a simulated space environment of simultaneous high vacuum and intense ultraviolet radiation, and then to high-energy electron radiation. The coatings were also subjected to simulated micrometeoroid impact (erosion). Measurements of spectral reflectance were obtained to determine the effects of these space simulations on the solar absorptance and thermal emittance of the coated surfaces. The coatings were also subjected to various tests to determine the physical characteristics of abrasion resistance, resistance to damage from thermal shock, and adherence of the coating to the substrate material under the condition of mechanical stress. The test coatings included: anodized aluminum blackened by use of two commercially available organic dyes; anodized aluminum blackened by inorganic compounds (dyes) of bismuth sulfide, cobalt sulfide, lead sulfide, and nickel sulfide; electrodeposition of nickel black on aluminum; one chemical-reaction-type coating for the blackening of stainless steel; one chemical-reaction coating on an inconel substrate; one chemical-reaction-type coating for blackening stainless steel or inconel; and a high-temperature black paint on both aluminum and inconel substrates.

The results of this investigation indicate that most of the black coatings experienced only negligible change of thermal radiation characteristics due to exposure to the simulated space environment. The only changes of solar absorptance noted were on the anodized aluminum samples dyed by use of commercial organic dyes and the inorganic compounds of bismuth sulfide and lead sulfide. Slight changes of thermal emittance were detected for the bismuth sulfide and nickel sulfide anodized aluminum and for the sodium dichromate blackened inconel. The greatest change of thermal emittance, 12.9 percent, was experienced by the black nickel plate.

INTRODUCTION

Black coatings were prepared and exposed to various simulated space environments to determine the effects of these environments on the spectral reflectance over the wavelength range from 0.25 μm to 25.0 μm. The relative flatness of the spectral reflectance was also investigated to determine whether the coatings could be used as flat absorbers for spacecraft or in ground-test space-simulation facilities. The spectral reflectance was numerically integrated to determine the effects of the simulated space environments on the overall value of solar absorptance and thermal emittance. The simulated environments included exposure of the coated specimens to electron radiation, micrometeoroid impact, and simultaneous high-vacuum and high-intensity ultraviolet radiation.

Further investigations were conducted to evaluate the coating integrity or mechanical properties. These investigations included an abrasive grit blast to determine abrasion resistance, thermal shock tests, and a test to indicate the flexibility and adherence of the coatings.

The coatings included in this report are: anodized aluminum blackened by use of two commercially available organic dyes; anodized aluminum blackened by inorganic dyes of bismuth sulfide (Bi_2S_3), cobalt sulfide (CoS), lead sulfide (PbS), and nickel sulfide (NiS); electrodeposition of nickel black on aluminum; one chemical-reaction-type coating for the blackening of stainless steel; one chemical-reaction-type coating on an inconel substrate; one chemical-reaction-type coating for blackening of stainless steel or inconel; and a high-temperature black paint on both aluminum and inconel.

The purpose of this paper is to present the methods of preparation, integrity or mechanical properties, and resistance to damage from the simulated space environments for each of the coatings.

Donald Humes conducted the tests of simulated micrometeoroid impact on the coated test samples and this phase of the investigation is discussed in an appendix.

Certain commercially available materials are identified in this paper to specify adequately the materials employed. In no case does this identification constitute an endorsement of these products by the National Aeronautics and Space Administration.

TEST SPECIMEN PREPARATION

Anodized Aluminum

Test samples were fabricated from commercially pure aluminum 1100 (2-S) 0.32 centimeter thick into 5.08-centimeter-radius semicircular disks. The samples

were then finished with 600 grit emery paper to obtain a relatively smooth surface free of mill scale or other surface contaminants.

The cleaning process which follows was to provide a clean surface for the coating application as well as to maintain an anodizing bath free of contamination by grease or other impurities. During the cleaning process and the subsequent coating processes, the test samples were handled in a manner to prevent contamination of the test surface. The samples were

(1) Vapor degreased by using trichloroethylene for a period of 30 minutes

(2) Rinsed in distilled water

(3) Immersed in an alkaline solution of trisodium phosphate and sodium carbonate for 5 minutes

(4) Rinsed in distilled water

(5) Immersed in a 50-percent nitric acid bath for 3 minutes

(6) Rinsed in distilled water

(7) Reacted in a bright dip bath for 3 to 5 minutes at 363° K

(8) Scrubbed with cotton swabs under running water to remove the smut formed by the bright dip bath, rinsed in distilled water, and then dried by a hot air blast.

During the anodizing process the aluminum specimen is made the anode in a suitable electrolytic bath. When a dc current is passed through the electrolytic bath a noncrystalline, porous, honeycomb structure of aluminum oxide is formed on the sample surface. The many variables of this process, such as the composition, concentration, and temperature of the electrolyte, the current density, and the bath time, all affect the character of the resulting anodic coating. The desired physical properties of the coating such as abrasion resistance, coating thickness, and porosity, will dictate the conditions of the anodizing process which is used. Much information on the anodizing of aluminum can be found in existing technical literature (see refs. 1 to 4) and the method ultimately selected for this investigation was the commonly used sulfuric acid process which produces the optimum coating for dyeing. The conditions used for this process were:

Electrolyte	15-percent sulfuric acid
Current density	0.1725 amp/cm^2
Temperature	302° K to 305° K
Time	60 to 120 minutes

To produce the black coating, the pores formed on the aluminum surface by the anodizing process must be impregnated with a coloring agent (or dye) which is then retained in the pores by a sealing process. For this investigation several types of dye

were used. (See table I.) Four of these dyes were inorganic substances whereas the other two were commercially available organic dyes of aniline derivatives. During the actual dyeing process by an inorganic dye, two solutions are used. When the test sample is immersed alternately in these solutions, a chemical reaction occurs which produces the dye inside the pores of the coating. This dye molecule is large with respect to the pore diameter and thus the pore is partially sealed by the dye process. In the case of the organic dye, the dye is simply absorbed by the pores.

In both cases, however, the dyed surface is sealed to render the coating nonabsorbing, impermeable, and thus stain resistant. There are many methods and substances which can be used to seal the dyed anodized coating and the method used will primarily depend on the intended application of the coated surface. The methods selected for the coatings in this investigation are shown in table I together with the dyeing process used. The water seal used for the inorganic Bi_2S_3, PbS, and NiS dyes produces a hydrated aluminum oxide with an accompanying increase in volume. This hydration and expansion effectively seals the dye within the pores of the anodized coating. The seal process used for the CoS inorganic dye and the two organic dyes was a nickel acetate, boric acid solution. The sealing action here is believed to be by precipitation of colloidal nickel hydroxide in the pores. The use of the boric acid in the sealant bath tends to reduce the possibility of the formation of a white film on the coating surface.

A simple test performed to determine whether a seal has been accomplished is described in reference 5. This test consists of placing a drop of anthraquinone violet RN on the test surface at room temperature for 5 minutes. If the resulting stain can then be removed by cleaning the surface with a detergent and water solution, a proper seal has been obtained. This test completed the preparation of the dyed anodized aluminum test samples.

Black Nickel Plate

The preliminary finishing and cleaning procedures of the aluminum test samples to be coated by this process were identical to those previously described for anodized coatings. The electrolyte and conditions of the electroplating bath as obtained from reference 6 were:

Electrolyte:

Nickel sulfate, 97.4 grams/liter
Sodium thiocyanate, 74.9 grams/liter
Zinc sulfate, 45.0 grams/liter
Lead acetate, 11.3 grams/liter

Operating conditions:

pH 6.3 to pH 6.7 (colorimetric)
Temperature, 296° K to 311° K
Current density, 10.76 to 21.53 amp/meter^2
Voltage, 0.75 to 1.5 volts
Time, 20 minutes
Anode, nickel

After plating, the samples were rinsed in distilled water and air dried and the preparation of the test samples was completed.

Du-Lite 3-0

The preliminary preparation of type 304 stainless steel for coating by the Du-Lite process required "vapor blasting" of the substrate, a blasting process which used -325 mesh aluminum oxide in a water suspension at a pressure of 5.17×10^5 to 5.51×10^5 newtons/meter^2 (75 to 80 psi) and at a distance of 10 to 15 centimeters from the sample. All substrates were cleaned prior to coating by the following process:

(1) Vapor degreased with trichloroethylene

(2) Immersed in alkaline cleaner (Du-Lite #45) at 363° K to 373° K for 7 to 8 minutes

(3) Washed in hot running water

(4) Immersed in (Aldak) cleaner at 386° K for 30 minutes

(5) Washed in hot running water

(6) Air dried

The Du-Lite 3-0 blackening process is a chemical conversion process where the substrate surface is coated with a combination of oxides formed by chemical reaction between the Du-Lite solution and substrate material. Test samples were prepared by the Lewis Research Center by using the process of the Du-Lite Chemical Corporation as follows:

(1) Immerse samples in Du-Lite 3-0 activator solution with a concentration of 337.5 grams/liter for 5 to 6 minutes at 363° K

(2) Wash in hot running water

(3) Immerse samples in Du-Lite 3-0 blackening solution of 575 grams/liter concentration for 40 minutes at 391° K

(4) Wash in hot running water

(5) Air dry

This procedure completes the test sample preparation.

Westinghouse Black

Preliminary preparation of the inconel substrates to be blackened by the Westinghouse Black process requires only that the surface be free of oxides and grease. Therefore, after surface finishing through 600 grit emery paper, the samples were vapor degreased with trichloroethylene, rinsed in distilled water, and air dried. The sample coating as prepared by Westinghouse Electric Corporation consisted of coating the substrate material by normal paint-spraying techniques with a mixture of an organopolysiloxane resin, a butyl acetate solvent, and finely divided leafing-type aluminum powders as described in reference 7. Blackening of the coating was then accomplished by heating the coated sample in an inert atmosphere at a temperature of 1172° K for a period of 5 minutes. The blackening action appears to occur from a combination of decomposition products from the organopolysiloxane with the leafing aluminum powders. The formation of this black coating is therefore independent of the substrate material, the only requirement being that the melting point of the substrate be greater than 933° K; however, the optimum black coating is obtained at a temperature of 1172° K.

Sodium Dichromate Blackening

Preliminary preparation of inconel, Inconel X, and type 347 stainless-steel test samples to be blackened by sodium dichromate consisted of roughening of the surface by a 120 grit aluminum oxide grit blast at a distance of 15 to 20 centimeters and a pressure of 6.89×10^5 newtons/meter^2 (100 lb/in^2). This initial roughening has been found to be desirable to insure a uniform reproducible surface coating. After the roughening process, the samples were cleaned with a detergent and rinsed in distilled water. Prior to coating, the test samples were cleaned in an ultrasonic cleaner by using a detergent solution and vapor degreased with trichloroethylene for 30 minutes.

The blackening of the test sample is accomplished by a chemical conversion process where the sample surface is coated with black oxides, primarily a chromium oxide, produced by chemical reaction between the molten sodium dichromate and the substrate material. The blackening process used in this investigation was as follows:

(1) Cover the clean sample surface with sodium dichromate crystals and react in a clean furnace at a temperature of 700° K for 30 minutes

(2) Clean surface with detergent and water solution

(3) Rinse in distilled water and air dry

Experience has shown that the most uniform coating can be obtained by this process when the procedure listed is repeated rather than simply doubling the reaction time in the furnace. This effect is probably due to the exposure of the surface to unreacted sodium dichromate.

Painted Coatings

Included in the materials investigated was a refractory paint, Pyromark. Although the exact composition of this paint is not available from the manufacturer, X-ray diffraction revealed the presence of chromium oxide. The paint may also contain a small amount of graphite plus a silicate binder and an organic vehicle.

Substrates of 1100 aluminum and inconel were prepared for the Pyromark paint coating by initially roughening the surface, as recommended by the paint manufacturer, by using a grit blast of 120 grit aluminum oxide at a pressure of 6.89×10^5 newtons/meter^2 (100 lb/in^2) at a distance of 15 to 20 centimeters from the sample. All samples were cleaned prior to coating by the following procedure:

(1) Vapor degreased with Freon for 5 minutes

(2) Cleaned in an ultrasonic cleaner with a Freon solution for 5 minutes

(3) Vapor degreased with Freon for 5 minutes

The Pyromark paint was applied by standard paint-spraying techniques and the curing procedure was that recommended by the manufacturer. The Pyromark paint cure specified air drying for 2 hours followed by a baking at 394° K for 2 hours. This procedure was repeated for each successive coat until the desired coating thickness was obtained. The baking temperature was then gradually increased to 522° K and maintained at this temperature for 1 hour.

Reproducibility

One of the criteria of a useful thermal control surface is that the coating be capable of being prepared with reproducible thermal radiation characteristics. For this reason a preliminary check on the reproducibility of the solar absorptance was made by measuring the spectral reflectance over a wavelength range from 0.25 μm to 2.6 μm of several identically prepared samples of each coating to be evaluated. The solar absorptance was then calculated and these values are presented in table II.

APPARATUS AND TEST PROCEDURES

Simulated Space Environment

The apparatus used in this investigation for the simulation of a space environment of simultaneous high vacuum and high intensity ultraviolet radiation is shown in figure 1. The high vacuum apparatus shown in figure 1(a) consisted of a 0.03-meter^3 stainless-steel vacuum chamber, pumped by a 6-inch fractionating oil diffusion pump and backed by a mechanical pump with a free air pumping speed of 2.33 liters/sec. A liquid nitrogen cold trap and optical baffle together with a refrigerated cold cap on the diffusion pump tower limited oil backstreaming and prevented oil contamination of the test samples. A test conducted to determine any oil contamination was performed by measuring the reflectance of highly polished aluminum surfaces prior to and after exposure in the test chamber. No significant change of reflectance was observed and it was therefore concluded that oil backstreaming was negligible. Refrigeration was provided for the elastomer seals in the system to reduce seal outgassing and enable lower pressures to be obtained. The pump-down time of the system with test samples installed required approximately 1 hour to attain a vacuum below 1.33×10^{-4} newton/meter^2 (1×10^{-6} torr). The exposure of test samples to simultaneous high-vacuum and high-intensity ultraviolet radiation was conducted in a vacuum range of 1.33×10^{-5} newton/meter^2 (1.0×10^{-7} torr) to 1.33×10^{-6} newton/meter^2 (1.0×10^{-8} torr).

While in the vacuum chamber the test samples were irradiated by high-intensity ultraviolet radiation from an air-cooled mercury vapor lamp (B-H6) positioned inside the test chamber. This lamp, mounted on an electrode designed to provide air cooling of the lamp, was operated in a quartz tube projecting into the chamber as shown in figure 1(b). To eliminate the possible thermal effects on test samples due to heating by radiation from the mercury vapor lamp, the samples were mounted on water-cooled supports at a distance of 12.7 centimeters from the lamp and sample temperature was maintained below 373° K during exposure.

The spectrum of the mercury vapor lamp as obtained from the lamp manufacturer's data (ref. 8) consists mainly of emission bands that may be many times the level of the solar continuum and is actually a poor duplication of the solar ultraviolet spectral distribution. However, the assumption was made that if the lamp radiant energy below 0.40 μm was set equal to the total solar radiant energy below 0.40 μm, the same degradation of test samples would occur. This assumption was the basis for the calculation of equivalent solar radiation levels on the test surfaces. For the physical arrangement used in this investigation, the lamp irradiance on test samples for the spectral region from 0.22 μm to 0.40 μm was equivalent to ten times the solar irradiance (at 1 astronomical unit) over this same range. Thus, the illumination level is defined as 10 "ultraviolet solar

constants" or 10 "suns," and the intensity time product is defined as "equivalent sun hours" (ESH) of ultraviolet radiation. The lamp irradiance for various wavelength bands and a distance of 12.7 cm between lamp and sample is shown in figure 2; also shown for comparison is the equivalent solar irradiance of 10 ultraviolet suns. The choice of 0.40 μm as an upper limit is purely arbitrary but it is believed to represent the upper limit of damaging radiation for nearly all materials of interest. However, some materials may be particularly sensitive to certain regions of the ultraviolet spectrum and the results of ultraviolet exposure included in this report as equivalent sun hours must be considered with these limitations.

The effect of a simulated space environment on the test surfaces was determined by measurement of spectral reflectance over a wavelength range from 0.25 μm to 25.0 μm, by using a commercially available integrating sphere spectrophotometer for the solar region of the spectrum (0.25 μm to 2.6 μm) and a heated cavity reflectometer for the infrared region of the spectrum (3.0 μm to 25.0 μm). Solar absorptance was calculated by an energy-weighted method using the spectral distribution reported in reference 9 for the sun and the reflectance data obtained from the integrating sphere spectrophotometer. Thermal emittance was obtained in a similar manner with the spectral distribution of a theoretical 300° K blackbody and the reflectance data obtained from the heated cavity reflectometer. After the initial measurement of reflectance, test samples were exposed to the simulated space environment of simultaneous high vacuum and intense ultraviolet radiation for an extended period of time and solar reflectance measurements were repeated. After a second long term exposure to the simulated space environment, measurement of solar reflectance was again repeated.

Test samples previously exposed to simultaneous high vacuum and ultraviolet radiation were then irradiated by high energy electrons to determine the effects produced by addition of this space environment. The irradiation of test surfaces was performed in air with a beam of 1 MeV electrons by using a cascaded rectifier accelerator. This phase of the investigation consisted of irradiating each test sample for the following doses and dose rates:

Doses	Dose rates
10^{12} electrons/cm^2	3.27×10^9 electrons/cm^2-sec
10^{13} electrons/cm^2	3.27×10^9 electrons/cm^2-sec
10^{14} electrons/cm^2	3.275×10^{10} electrons/cm^2-sec
10^{15} electrons/cm^2	2.875×10^{11} electrons/cm^2-sec

Measurements of solar reflectance after each dosage were obtained to determine any changes of solar absorptance.

After exposure of the samples to the simulated space environments discussed previously, a final measurement of spectral reflectance over the wavelength range of 0.25 μm to 25.0 μm was obtained. However, prior to obtaining the final measurement of thermal emittance in the spectral region 3.0 μm to 25.0 μm, the samples had been stored for several months. The storage is not considered detrimental to the validity of the data for coatings of this type.

Simulation of the near-earth micrometeoroid environment and the effects on the spectral reflectance in the wavelength range of 0.25 μm to 25.0 μm for the coated test surfaces was obtained by bombarding test samples with many small iron fragments created when a shaped charge with a cylindrical cast iron liner was exploded. The shaped charge of high explosive, identical to that described in reference 10, imploded on the cast iron liner, crushed it into fragments ranging in size from 3 μm to 200 μm, and accelerated them to an initial velocity of 12 km/sec. The effect of the cratering damage on the thermal radiation characteristics of the coated test samples was determined by spectral reflectance measurements prior to and after the simulated micrometeoroid impact. Again, these samples were stored for several months prior to determining the final values of thermal emittance. The test procedures, calibration of test apparatus, and interpretation of test results are included in detail in the appendix of this report.

Integrity Testing

Abrasion resistance.- Before the abrasion resistance value of test coatings can be determined, the coating thickness must be known. The coating thickness for most of the coatings included in this investigation was measured by use of a commercially available nondestructive thickness gage. However, when the test surface is roughened, the accuracy of the instrument is greatly decreased and an alternate method consisting of sectioning the samples and measuring the coating thickness optically with a metallograph was used.

The abrasion resistance of the test coating was determined by use of the abrasive air blast apparatus described in reference 11. This apparatus consisted of an air pressure regulator and drying train, a manometer, a surge tank, a nozzle, and the test chamber.

Clean dry air at a pressure of 8.10×10^3 newtons/meter^2 (60 mm Hg) enters the nozzle and becomes thoroughly mixed with a 180 grit silicon carbide abrasive. This mixture then impinges on the test surface which is placed at an angle of 45^o and touches the nozzle opening. The specimen is observed throughout the test and when a 2 mm spot, which is an arbitrary end point for this test, is worn through the coating, the grit flow is stopped. The weight of the grit used to produce this spot is then determined and the abrasion resistance of the coating in terms of grams of abrasive per micrometers of coating thickness is calculated.

Thermal shock.- The apparatus used to determine the resistance to damage from thermal shock of the coated test samples consisted of a bank of quartz tube radiators as a heat source and a Dewar flask of liquid nitrogen as a heat sink. Thermocouples attached to the test samples were used to indicate maximum temperature. A stop watch was used to obtain the rates of temperature changes. The test procedure consisted of heating the test sample to a temperature of 478° K while timing the temperature rise. The sample after reaching temperature was then immediately immersed in a Dewar flask of liquid nitrogen, and the time required for the sample temperature to reach that of the nitrogen was noted. Photomicrographs at a magnification of $\times$ 70 were made of the sample surfaces prior to thermal shock, after the first cycle, and after the tenth cycle.

Coating adherence.- The apparatus and procedures used for this investigation were variations of the A.S.T.M. "Free Bend Test" method used to determine the ductility of materials and described in reference 12. The test was intended to subject the test coatings to a relatively severe stress as an aid in evaluating the adherence of the coating to the substrate material. The test consisted of producing an initial bend within the gage length on the sample as shown in figure 3(a). After this initial bend of approximately 30°, the test sample is treated as a strut and a compressive force is applied to the ends of the sample as shown in figure 3(b). During this bending the test sample is observed and the test was concluded when failure of the coating occurred. The angle of the final bend, bend radius, and visual appearance of the test section gave an indication of the adherence of the coating.

RESULTS AND DISCUSSION

Simulated Space Environment

The effects of exposure to a simulated space environment of simultaneous high vacuum and ultraviolet radiation and then added electron radiation of 10^{15} electrons/cm^2 on the thermal radiation characteristics of the test samples are shown in figure 4. Values of solar reflectance were obtained to determine changes after each exposure to the vacuum and ultraviolet radiation and also after each dose of electron radiation. Values of thermal emittance for the samples were obtained prior to the first test and after the last dose of electron radiation. The calculated values of solar absorptance and thermal emittance shown in figure 4 are also given in table III for convenience in comparison of the data.

The measurements of spectral reflectance were made, as described in a preceding section, in a normal air atmosphere after removal of the samples from the simulated space environment test chamber. The high-energy electron irradiation of the samples was conducted in an air atmosphere after exposure of the samples to high vacuum and

ultraviolet radiation. This method of space environment simulation may not indicate the synergistic effects which could possibly result from a simultaneous exposure to all space environment parameters; however, it is believed that the results obtained are indicative of the effects of a space environment on the black coatings tested.

Anodized aluminum.- Spectral reflectance curves together with the solar absorptance and thermal emittance values are shown in figures 4(a) to 4(f) for the anodized aluminum samples. The initial values of solar absorptance for the dyed anodized aluminum samples proved to be relatively low except for the NiS and CoS dyed surfaces which had initial values of 0.970 and 0.957, respectively. The initial values of room-temperature emittance for these samples all proved to be fairly high, the values ranging from 0.909 for the Bi_2S_3 dyed surface to 0.930 for the CoS dyed surface.

After an initial exposure to the simulated space environment of simultaneous high vacuum and ultraviolet radiation, the surfaces dyed by the organic compounds as well as those dyed with Bi_2S_3 and PbS all show a slight increase of solar absorptance. This increase is due to the dulling of the original glossy surface caused by the combination of high vacuum, ultraviolet radiation, and the thermal effects resulting from heating of the samples to near 373° K. The inorganic dyed coatings of NiS and CoS showed no change of solar absorptance for exposures of 1540 ESH and 1760 ESH, respectively. After a second exposure to this simulated space environment for an additional 2000 ESH, there was no further significant change in the solar absorptance for any of the test surfaces. Measurements of spectral reflectance of the test surfaces after irradiation by high-energy electrons for a total dose of 10^{15} electrons/cm^2 indicate no change from the previously measured values. Values of thermal emittance obtained from the measured spectral reflectance data show only a negligible change of 2.1 percent and 2.9 percent for the Bi_2S_3 and NiS dyed surfaces as a result of exposure to the simulated space environment.

The results of these tests indicate that the thermal radiation characteristics of several of these dyed anodized black coatings may be slightly altered by prolonged exposure to a simulated space environment. The NiS and CoS dyed coatings, however, proved to be stable with relatively high absorptance values over the entire wavelength region considered. The Bi_2S_3 inorganic dyed surface proved to be somewhat unstable and also proved to be the least reproducible dyed coating investigated. These factors together with the relatively low absorptance values make the Bi_2S_3 coating somewhat undesirable as a high absorber for space applications. The organic dyed surfaces (Sandoz OA and Sandoz BK) as well as the inorganic PbS dye all show slight changes of solar absorptance when exposed to the simulated space environment for prolonged periods and all have relatively low values of solar absorptance which limit their usefulness as high absorber surfaces.

Black nickel plate.- Spectral reflectance curves for black nickel plate as well as solar absorptance and thermal emittance values are shown in figure 4(g). This coating

proved to be very stable over the solar region of the spectrum for exposures to a simulated space environment of simultaneous high vacuum and ultraviolet radiation of 3800 ESH plus electron radiation of 10^{15} electrons/cm^2, and showed no significant change of solar absorptance from the initial high value of 0.959. However, the room-temperature emittance at the longer wavelengths (from 3 μm to 25 μm) was relatively low, 0.686, and was reduced even further to 0.598 by exposure to the simulated space environment. This 12-percent change of thermal emittance was the largest of any of the black coatings tested.

Chemical reaction coatings.- Spectral reflectance curves for the chemical-reaction-type coatings are shown in figures 4(h) to 4(l) together with the calculated solar absorptance and thermal emittance values. These coatings include the Du-Lite 3-0 coating, the Westinghouse blackening process, and the sodium dichromate blackening of stainless steels (or inconel). The data indicate that these coatings are good flat absorbers in the solar spectral region. The initial values of solar absorptance for the surfaces are all relatively high, and range from 0.963 for the sodium dichromate blackened Inconel X to 0.925 for the sodium dichromate blackening of type 347 stainless steel. However, the thermal emittance of these surfaces is relatively low, the lowest value being 0.565 for the type 347 stainless steel blackened with sodium dichromate. The relatively low values of thermal emittance obtained for the sodium dichromate blackened surfaces are due to the very thin coatings, which are probably semitransparent in the long wavelength region of the spectrum. These coatings generally proved to be very stable during exposure to a simulated space environment. The only significant changes noted were changes of the thermal emittance for the Du-Lite 3-0 coating on type 304 stainless steel and the sodium dichromate blackened inconel which were 4.1 percent and 2.7 percent, respectively. These changes are probably negligible for applications where these surfaces may be considered. The major disadvantage of the sodium dichromate blackened coatings and the Westinghouse black coating may be the relatively high temperatures required during the coating process.

Painted surface.- The spectral reflectance characteristics for the high-temperature black paint included in this investigation are shown in figures 4(m) and 4(n). Although it is obvious that the reflectance for this paint cannot be considered as flat, the calculated values of solar absorptance and thermal emittance are relatively high. Furthermore, the paint is virtually unaffected by prolonged exposure to the simulated space environment, and thus retains the initially high values of solar absorptance and thermal emittance. (See figs. 4(m) and 4(n) and table III.)

Micrometeoroid Erosion

The effects of micrometeoroid erosion on the thermal radiation characteristics of spacecraft thermal control surfaces should be included when the space environment is

considered. However, the difficulty in accurately simulating this parameter as well as the uncertainty in the actual space environment suggested that this phase of the investigation be considered separately.

The test procedures and evaluation of cratering damage sustained by the test samples when exposed to a simulated near-earth micrometeoroid environment was determined by the methods described in detail in the appendix. The results of this investigation indicate that the time in a space micrometeoroid environment required to damage the test samples as extensively as the simulation method is in excess of 10^{10} seconds or over 300 years.

Calculated values of solar absorptance and thermal emittance prior to and after simulated micrometeoroid impact are given in table IV. Changes of the thermal emittance or solar absorptance of the test surfaces due to exposure of the samples to micrometeoroid impact can generally be attributed to one of two different effects. Generally, increases are noted when the surface has been roughened with little or no removal of the black coating (usually noted for the thick coatings). Decreases are usually obtained when there is considerable spalling of the coating, and thus the substrate surface is exposed. The data show that the changes of solar absorptance due to the cratering damage produced by the simulation are less than 3 percent for all coatings tested. The changes of thermal emittance, however, were considerably more variable, and ranged from a nearly 21-percent change for the black nickel plate to no change for the dyed anodized aluminum surfaces. These changes of solar absorptance and thermal emittance are felt to be negligible when the equivalent time in a space environment is considered; therefore, the results indicate that none of the test surfaces are appreciably affected by the micrometeoroid environment.

Integrity Tests

The results of the various tests conducted to determine the integrity of the coated test samples are shown in table V.

Abrasion resistance.- The evaluation of the measured abrasion resistance as determined by the methods used in this investigation is limited by the nonexistence of established standards. Thus, the results must be presented as a comparison of the surfaces included in the test program. The abrasion resistance values given in table V indicate that the coatings which appear to be most durable are the anodized aluminum surfaces which had values ranging from 10.35 grams/μm to 14.15 grams/μm. The lowest values of abrasion resistance were found for the sodium-dichromate-blackened stainless steels and varied from approximately 0.21 gram/μm to 0.42 gram/μm.

Thermal shock.- No failure of the test coatings due to peeling or spalling was observed during the test for resistance to damage from thermal shock. However,

examination of the test samples under 70 power magnification showed that the NiS and CoS dyed anodized aluminum surfaces had a crazed appearance prior to thermal shock, as shown in figure 5(a). After the first cycle of thermal shock, all test surfaces were re-examined and it was noted that all anodized surfaces were now crazed, and that the previously observed crazing of NiS and CoS dyed surfaces had been accentuated by the appearance of more cracks. This crazing was not observed for any of the other types of test coatings. Subsequent cycling for nine additional cycles had no further effects on the anodized surfaces. The photomicrographs in figure 5 are representative of the effects due to thermal cycling observed for all test surfaces. It was felt that the crazing of the anodized surfaces may have an effect on the adherence of the coating or change the spectral reflectance but measurements of spectral reflectance and bend tests made prior to and after thermal shock proved that this was not the case.

Flexibility (adherence).- The results of the bend test, as shown in table V, indicate that all the test coatings are very adherent and no failure of the coating occurred within reasonable limits of bend angles, although for the test the samples were in tension only. (See fig. 3.) As stated previously, it was felt that the crazing induced by the thermal cycling of the anodized test samples may have an effect on the coating adherence. Therefore, samples that had been subjected to thermal cycling were also subjected to the bend test. It is apparent that in most cases the only effect was to increase the maximum bend angle before failure. In general, most of the coatings included in this investigation possess physical properties which may insure reliability as spacecraft thermal control surfaces or as coatings for ground-test simulation facilities.

CONCLUDING REMARKS

The results of the investigation on the effects of a simulated space environment on high absorber (black) coatings indicate that the thermal radiation characteristics of certain types of black coatings may be altered slightly by prolonged exposures to an environment of simultaneous high vacuum and ultraviolet radiation. Of the coatings investigated, results show that many of the coatings are virtually unaffected by the simulated space environment.

High-energy electron radiation, for doses up to 10^{15} electrons/cm^2, appears to have no effect on the radiation characteristics of the black coatings tested when added to damage previously indicated because of approximately 5 equivalent months of simulated solar ultraviolet radiation.

Exposure of the test surfaces to a simulated near-earth micrometeoroid environment (for reasonable lengths of time) will produce no significant change in the thermal radiation characteristics of the black coatings included in this investigation.

The physical properties of the coatings included in this investigation (coating adherence, resistance to abrasion, and resistance to damage from thermal shock) were found to be suitable for applications such as highly absorbing space vehicle surfaces or as coatings for ground-test space simulation facilities.

One disadvantage of some of the black coatings tested is the comparatively complex preparation of the coating. In two cases (Westinghouse Black, and sodium dichromate blackening), the requirement of relatively high temperatures during preparation was a disadvantage.

Langley Research Center,
National Aeronautics and Space Administration,
Langley Station, Hampton, Va., January 24, 1967,
124-09-18-05-23.

APPENDIX

MICROMETEOROID IMPACT SIMULATION TESTS ON HIGH ABSORBER COATINGS FOR THE SPACE ENVIRONMENT

By Donald H. Humes

The micrometeoroid test samples consisted of black coatings which ranged in thickness from 3 μm on some samples to 30 μm on others, on substrate materials of type 1100 aluminum, type 347 stainless steel, type 304 stainless steel, inconel, and Inconel X. The substrate materials and the finished samples had surface finishes rougher than 3 μm root mean square. The samples were semicircular in shape with a 5.08-cm radius; however, the area on which the pre-test spectral reflectance measurements were made was a circular area approximately 2 cm in diameter.

The test procedure consisted of mounting the semicircular test sample and a semicircular copper control sample together in the target holder 43 cm from the shaped charge. A tetryl booster charge and detonator were attached to the shaped charge and exploded. The test sample and shaped charge were in air during the test since preliminary tests showed that a black film was deposited on the test samples when the test was attempted in a vacuum enclosure. Because of the drag that the iron particles experienced while traveling through the air, the velocity was undoubtedly reduced from the original velocity of 12 km/sec by the time they struck the test samples. However, the actual impact velocity was not needed to determine the effective exposure time of the samples in the space environment.

The cratering damage produced on the test samples could not be obtained directly since the craters did not show up well on the coated surface when viewed through a microscope. Therefore, one uncoated sample of each substrate material was subjected to bombardment by the iron particles from the shaped charge. The damage that resulted is shown in figure 6, where the cumulative number of craters per square meter is plotted as a function of the crater size. The crater sizes observed in the uncoated stainless-steel, inconel, and Inconel X samples ranged between 37 μm in diameter to 260 μm in diameter as indicated by the solid vertical lines. Similarly, the dashed vertical lines indicate the range of craters sizes observed in the aluminum sample were 37 μm to 370 μm in diameter. The total number of craters per square meter was approximately 1.2×10^6 in each case. The good agreement in the number of craters formed on the samples and on the size distribution of the craters is considered evidence of the reproducibility of the shaped charge accelerator. The percentage of the area affected by the craters was calculated by summing the areas of all the craters. The summation was made by fairing a straight line through the data in figure 6, obtaining an equation for the straight

line, and integrating. The results depend on how the line is faired through the data since the data points do not fall on one straight line. By using rather extreme fairings to define the possible range, it was determined that between 0.3 and 1 percent of the stainless-steel, inconel, and Inconel X surface area was affected by craters, and that between 0.4 and 1.2 percent of the surface of the aluminum sample was affected.

The test samples which had thin coatings (less than 15 μm thick) were assumed to receive the same damage as the substrate material received in figure 6. Because the resistance to micrometeoroid penetration of thick coating materials is probably more like aluminum than stainless steel or inconel, the test samples which had thick coatings (greater than 15 μm thick) were all assumed to receive the same damage as the aluminum target in figure 6. It should be noted that opposite effects on spectral reflectance should be expected when thin and thick coatings are compared. When the coating is thin, the particles will penetrate the coating, crater in the substrate, expose the shiny substrate material, and increase the reflectance. When the coating is thick, most of the particles will produce craters in the coating material, make the surface rougher but not expose the substrate material, and therefore decrease the reflectance.

Two steps were taken to assure that no gross error was made in assuming that the test samples experienced the same environment as the four samples used to obtain figure 6. The steps were (1) counting the total numbers of craters on several randomly chosen areas on each of the copper control samples and (2) counting the number of large craters on several randomly chosen areas on each of the test samples. The first step showed that the percent of surface area affected by the craters varied from 0.1 to 1.2 percent, which is slightly larger than the variation in the four samples used to obtain figure 6. The second step showed that the number of large craters on the test samples varied by no more than a factor of ten.

The damage that would have been produced on the samples had they been placed in a near-earth orbit was calculated by considering the Explorer XVI and Explorer XXIII micrometeoroid satellite data. If it is assumed that meteoroids produce hemispherical craters and that the conversion factor from quasi-infinite penetration to the maximum finite thickness penetrated is 1.5, it follows that the micrometeoroids which penetrated the stainless-steel sensors of thickness t on Explorer XXIII would have produced craters of diameter $4t/3$ or larger on a stainless-steel plate. For instance, the 0.025-mm-thick sensors on Explorer XXIII had a penetration flux of 4.5×10^{-6} $m^{-2}sec^{-1}$. (See ref. 13.) Therefore, the rate at which 0.034-mm-diameter craters or larger would be produced on a stainless-steel plate is also 4.5×10^{-6} $m^{-2}sec^{-1}$. This data point is plotted in figure 7(a). Another data point obtained from the 0.051-mm-thick sensors on explorer XXIII is also shown. The maximum likelihood slope from the Explorer XVI data (ref. 14) which is for 0.025-mm-, 0.051-mm-, and 0.127-mm-thick beryllium copper

sensors is plotted through the data points from Explorer XXIII. It is felt that this slope should apply to the Explorer XXIII data since the penetration flux of the 0.025- and 0.051-mm sensors on both of these Explorer satellites was nearly identical. The range of crater diameters of interest in this study greatly exceeds the range covered by the Explorer XVI and Explorer XXIII satellites. Therefore, the curve through the data must be extrapolated to smaller and to larger crater diameters. The range of crater diameters of interest is from about 1 μm to 1 mm in diameter. Craters smaller than 1 μm in diameter will not affect the thermal properties of the coatings because the surface roughness and thickness of the coatings exceeded 3 μm. Craters larger than 1 mm in diameter are considered to be out of the region of erosion and into the region of major structural damage. Certainly, this upper limit was selected arbitrarily and it does affect the results obtained; however, increasing the range of interest another order of magnitude to include those craters 10 mm in diameter is unreasonable for erosion studies. Furthermore, craters larger than 1 mm in diameter should be rare, an exposure of 4.22×10^7 m^2s would result in only one such crater according to figure 7(a).

The percentage of the area of stainless-steel samples affected by micrometeoroid craters, resulting from exposure to the micrometeoroid environment shown in figure 7(a), was calculated by summing the areas of all the craters. The summation was made by obtaining an equation for the straight line, and integrating.

The damage that would have been produced on an aluminum plate was calculated in a similar manner. First, the effective thickness of aluminum which the stainless-steel sensors represented was calculated by using the Herrmann and Jones penetration equation (ref. 15). This equation gives a greater difference in penetration resistance, a factor of 2.5, than the Charters and Summers equation (ref. 16). The satellite slope was drawn through the adjusted satellite data. The resulting model of micrometeoroid cratering damage is shown in figure 7(b).

The photomicrographs of figure 8 showing the effects of simulated micrometeoroid environment on surfaces are typical of the cratering observed for all the test samples included in this investigation. It was observed on the Pyromark-painted test surface that the simulated micrometeoroid impacts had caused spalling of the coating around the edge of the craters and had exposed areas of the substrate material much greater than the area of the crater itself.

The percent of the sample which would be marred by craters is shown in figure 9 as a function of the exposure time in the model environment. It can be seen from figure 9 that the time in space required to damage the samples as extensively as the shaped charge did is in excess of 10^{10} seconds (300 years).

REFERENCES

1. Wernick, S.; and Pinner, R.: The Surface Treatment and Finishing of Aluminum and Its Alloys. Second ed., Robert Draper Ltd., c.1959.

2. Stiller, Frank P.: Coloring Anodized Aluminum. Metal Finishing Guidebook Directory, 26th ed., Finishing Publ., Inc., c.1957, pp. 496-502.

3. Keller, F.; Hunter, M. S.; and Robinson, D. L.: Structural Features of Oxide Coatings on Aluminum. J. Electrochem. Soc., vol. 100, 1953, pp. 411-419.

4. Kissin, G. H., ed.: The Finishing of Aluminum. Reinhold Publ. Corp., c.1963.

5. Anon.: Tentative Method of Test for Resistance of Anodically Coated Aluminum to Staining by Dyes. ASTM Designation: B 136 – 63 T. Issued 1963.

6. Marinaro, A. T.; and Packman, Louis: Black Nickel Plating. Metal Finishing Guidebook Directory, 26th ed., Finishing Publ., Inc., c.1957, pp. 391-393.

7. Rohrer, Kenneth L.: New Black Emissivity Coating. Mater. Design Eng., vol. 56, no. 2, Aug. 1962, pp. 110-112.

8. Anon.: High Brightness Mercury Arc Lamps Capillary Type A-H6 and B-H6 Application Data and Accessory Equipment. GET-1248H, Outdoor Lighting Dept., Gen. Elec. Co., Feb. 1961.

9. Johnson, F. S.: The Solar Constant. J. Meteorol., vol. 11, no. 6, Dec. 1954, pp. 431-439.

10. Gehring, John W., Jr.: An Analysis of Micro-Particle Cratering in a Variety of Target Materials. Proceedings of the Third Symposium on Hypervelocity Impact, Vol. 1, F. Genevese, ed., Armour Res. Found., Illinois Inst. Technol., Feb. 1959, pp. 61-80.

11. Schuh, A. E.; and Kern, E. W.: Measurement of Abrasion Resistance. I – Paints, Varnishes, and Lacquers. Ind. Eng. Chem., Anal. Ed., vol. 3, no. 1, Jan. 15, 1931, pp. 72-76.

12. Mapes, F. S.: Bend Tests for Ductile Metals. Metals Handbook, Taylor Lyman, ed., Am. Soc. Metals, c.1948, pp. 124-125.

13. O'Neal, Robert L., compiler: The Explorer XXIII Micrometeoroid Satellite. Description and Preliminary Results for the Period November 6, 1964 Through February 15, 1965. NASA TM X-1123, 1965.

14. Hastings, Earl C., Jr., compiler: The Explorer XVI Micrometeoroid Satellite-Supplement III, Preliminary Results for Period May 27, 1963 Through July 22, 1963. NASA TM X-949, 1964.

15. Herrmann, Walter; and Jones, Arfon H.: Survey of Hypervelocity Impact Information A.S.R.L. Rept. 99-1, Massachusetts Inst. Technol., Sept. 1961. (Available from ASTIA as Doc. AD 267 289.)

16. Summers, James L.; and Charters, A. C.: High Speed Impact of Metal Projectiles in Targets of Various Materials. Proceedings of the Third Symposium on Hypervelocity Impact, Vol. 1, F. Genevese, ed., Armour Res. Found., Illinois Inst. Technol., Feb. 1959, pp. 101-110.

TABLE I.- COLORING AND SEALING PROCEDURES FOR ANODIZED ALUMINUM COATINGS

Dye	Type	Anodizing time, min	Coloring procedure						Sealing procedure				
			Dip	Solution	Concentration, g/l	Temperature, °C	pH	Time, min	Solution	Concentration, g/l	pH	Temperature, °C	Time, min
Bismuth sulfide, Bi_2S_3	Inorganic	60	1st	Bismuth nitrate (in acetone)	420	24		Repeated alternate dips of 3 to 5 min	Water		5.5 to 5.8	90.5 to 93.3	10
			2d	Ammonium hydrosulfide	30	24							
Cobalt sulfide, CoS	Inorganic	120	1st	Cobalt acetate	200	43 to 49	6.2	15	Nickel acetate	5	5.5 to 5.8	90.5 to 93.3	10
			2d	Ammonium hydrosulfide	30	24		5 to 15	Boric acid	5			
Nickel sulfide, NiS	Inorganic	120	1st	Nickel acetate	50	24	6	Repeated alternate dips of 2 to 3 min until black	Water		5.5 to 5.8	90.5 to 93.3	10
			2d	Ammonium hydrosulfide	Concentrated	24							
Lead sulfide, Pbs	Inorganic	120	1st	Lead acetate	50	43 to 49	5.95	Repeated alternate dips of 5 min. Swab surface while in 2d dip	Water		5.5 to 5.8	90.5 to 93.3	10
			2d	Ammonium hydrosulfide	30	24							
Sandoz black BK	Organic (aniline derivative)	60		Sandoz black BK	10	65.5	7.4	30	Nickel acetate	5	5.5 to 5.8	90.5 to 93.3	10
									Boric acid	5			
Sandoz black OA	Organic (aniline derivative)	60		Sandoz black OA	10	65.5	6.0	30	Nickel acetate	5	5.5 to 5.8	90.5 to 93.3	10
									Boric acid	5			

TABLE II.- SAMPLE REPRODUCIBILITY OF SOLAR ABSORPTANCE α_s

Sample coating	Substrate	Sample number for -			Average α_s
		1	2	3	
		α_s	α_s	α_s	
Bi_2S_3 dyed anodized Al	1100 (2-S) Al	*0.755	0.754	0.728	0.746
CoS dyed anodized Al	1100 (2-S) Al	.950	.958	.957	.955
NiS dyed anodized Al	1100 (2-S) Al	.976	.966	.970	.971
PbS dyed anodized Al	1100 (2-S) Al	.876	.878	.861	.872
Sandoz black BK dyed anodized Al	1100 (2-S) Al	.761	.774	.757	.764
Sandoz black OA dyed anodized Al	1100 (2-S) Al	.655	.664	.647	.655
Black nickel plate	1100 (2-S) Al	.951	.957	.959	.956
Du-lite 3-0	Type 304 stainless-steel grit blasted	.936	.941	.952	.943
Westinghouse black	Inconel	.914	.927		.920
$Na_2Cr_2O_7$ blackened	Type 347 stainless steel	.925	.934	.928	.929
$Na_2Cr_2O_7$ blackened	Inconel	.951	.946	.956	.951
$Na_2Cr_2O_7$ blackened	Inconel X	.963	.948	.954	.955
Pyromark black	1100 (2-S) Al	.909	.907	.902	.906
Pyromark black	Inconel	.906	.903	.906	.905

*Precision of measurement is ±0.01 absolute.

TABLE III.- EFFECTS OF THE SPACE SIMULATION ENVIRONMENT (SSE) OF HIGH VACUUM, ULTRAVIOLET RADIATION AND ELECTRON RADIATION ON SOLAR ABSORPTANCE α_S AND THERMAL EMITTANCE ϵ_T

Sample coating	Substrate	Initial α_S	Initial ϵ_T	Equivalent sun hours of ultraviolet in vacuum (*)	α_S after space simulation environment and 10^{15} electrons/cm^2	Total percent change of α_S	ϵ_T after space simulation environment and 10^{15} electrons/cm^2	Total percent change of ϵ_T
Bi_2S_3 dyed anodized Al	1100 (2-S) Al	0.728	0.909	3540	0.760	**4.4	0.890	2.1
CoS dyed anodized Al	1100 (2-S) Al	.957	.930	3760	.963	Negligible	.924	Negligible
NiS dyed anodized Al	1100 (2-S) Al	.970	.929	3540	.972	Negligible	.902	2.9
PbS dyed anodized Al	1100 (2-S) Al	.861	.912	3540	.891	3.5	.908	Negligible
Sandoz black BK dyed anodized Al	1100 (2-S) Al	.757	.926	3540	.786	3.7	.929	Negligible
Sandoz black OA dyed anodized Al	1100 (2-S) Al	.647	.927	3540	.684	5.7	.913	Negligible
Black nickel plate	1100 (2-S) Al	.959	.686	3800	.953	Negligible	.598	12.8
Du-lite 3-0	Type 304 stainless-steel grit blasted	.952	.653	3800	.945	Negligible	.626	4.1
Westinghouse black	Inconel	.927	.822	4930	.928	Negligible	.816	Negligible
$Na_2Cr_2O_7$ blackened	Type 347 stainless steel	.925	.565	3980	.922	Negligible	.564	Negligible
$Na_2Cr_2O_7$ blackened	Inconel	.951	.840	4770	.959	Negligible	.817	2.7
$Na_2Cr_2O_7$ blackened	Inconel X	.963	.806	2560	.960	Negligible	.808	Negligible
Pyromark black	1100 (2-S) Al	.902	.830	3440	.903	Negligible	.820	Negligible
Pyromark black	Inconel	.906	.842	3440	.906	Negligible	.845	Negligible

*The high vacuum and ultraviolet radiation were simultaneous.

**Precision of measurement is ±0.01 absolute.

TABLE IV.- EFFECTS OF SIMULATED MICROMETEOROID IMPACT ON SOLAR ABSORPTANCE α_s AND THERMAL EMITTANCE ϵ_T

Sample coating	Substrate	Initial α_s	Final α_s after micrometeoroid impact (**)	Percent change of α_s	Initial ϵ_T	Final ϵ_T after micrometeoroid impact	Percent change of ϵ_T
Bi_2S_3 dyed anodized Al	1100 (2-S) Al	*0.754	0.743	Negligible	0.909	0.917	Negligible
CoS dyed anodized Al	1100 (2-S) Al	.958	.962	Negligible	.930	.936	Negligible
NiS dyed anodized Al	1100 (2-S) Al	.966	.965	Negligible	.929	.933	Negligible
PbS dyed anodized Al	1100 (2-S) Al	.878	.881	Negligible	.912	.908	Negligible
Sandoz black BK dyed anodized Al	1100 (2-S) Al	.774	.796	2.8	.926	.929	Negligible
Sandoz black OA dyed anodized Al	1100 (2-S) Al	.664	.681	2.6	.927	.915	Negligible
Black nickel plate	1100 (2-S) Al	.957	.956	Negligible	.686	.828	20.7
Du-lite 3-0	Type 304 stainless-steel grit blasted	.941	.944	Negligible	.653	.639	2.1
Westinghouse black	Inconel	.914	.924	Negligible	.822	.718	12.6
$Na_2Cr_2O_7$ blackened	Type 347 stainless steel	.930	.904	2.8	.565	.603	6.7
$Na_2Cr_2O_7$ blackened	Inconel	.956	.930	2.7	.840	.730	13.1
$Na_2Cr_2O_7$ blackened	Inconel X	.954	.932	2.3	.806	.785	2.6
Pyromark black	1100 (2-S) Al	.907	.923	1.8	.830	.873	5.2
Pyromark black	Inconel	.903	.921	2.0	.842	.866	2.8

*Precision of measurement is ±0.01 absolute.

**The micrometeoroid flux is equivalent to 300 years in an orbit comparable to Explorer XVI and XXIII.

TABLE V.- RESULTS OF COATING INTEGRITY TESTS

Sample coating	Substrate	Abrasion resistance		Thermal shock test			Flexibility (bend) test					
							Before thermal shock			After thermal shock		
		Coating thickness, μm	Abrasive resistance, g/μm	Heating rate, ^{o}K/sec (*)	Cooling rate, ^{o}K/sec (**)	Number of cycles	Maximum angle, deg	Bend radius, mm	Remarks	Maximum angle, deg	Bend radius, mm	Remarks
Bi_2S_3 dyed anodized Al	1100 (2-S) Al	26.4	13.37	6.0	11.4	10	78	26	Some macroscopic cracks	130	18	Some macroscopic cracks
CoS dyed anodized Al	1100 (2-S) Al	26.2	14.15	7.7	10.8	10	86	18	Some macroscopic cracks	166	8	Some macroscopic cracks
NiS dyed anodized Al	1100 (2-S) Al	23.1	10.85	8.9	11.8	10	110	14	Some macroscopic cracks	147	10	Some macroscopic cracks
PbS dyed anodized Al	1100 (2-S) Al	17.3	12.77	7.9	11.8	10	87	14	Some macroscopic cracks	160	10	Some macroscopic cracks
Sandoz black BK dyed anodized Al	1100 (2-S) Al	22.6	10.35	4.9	11.1	10	82	22	Some macroscopic cracks	120	10	Some macroscopic cracks
Sandoz black OA dyed anodized Al	1100 (2-S) Al	20.1	12.72	4.1	10.5	10	75	15	Some macroscopic cracks	87	15	Some macroscopic cracks
Black nickel plate	1100 (2-S) Al	2.8	2.20	9.4	11.4	10	127	14	Slight spalling at edges	121	18	Some macroscopic cracks and some spalling
Du-lite 3-0	Type 304 stainless-steel grit blasted	3.8	.51	7.6	10.9	10			No specimens available	180	7	No effects
$Na_2Cr_2O_7$ blackened	Type 347 stainless steel	7.6	.26	6.8	11.2	10	180	4	Many macroscopic cracks	180	4	Many macroscopic cracks
$Na_2Cr_2O_7$ blackened	Inconel	9.6	.21	4.4	10.6	10	180	5	Many macroscopic cracks	180	5	Many macroscopic cracks
$Na_2Cr_2O_7$ blackened	Inconel X	4.8	.42	4.2	10.4	10	180	5	Many macroscopic cracks	180	5	Many macroscopic cracks
Pyromark black	1100 (2-S) Al	32.8	1.26	5.8	8.9	10	180	8	Some macroscopic cracks	119	22	Many macroscopic cracks
Pyromark black	Inconel	32.3	1.26	5.5	10.5	10	180	5	Some macroscopic cracks	180	11	Many macroscopic cracks

*Maximum temperature used 478^{o} K, obtained by heating specimen in air with quartz glow tubes.

**Minimum temperature used 78^{o} K, obtained by quenching specimen immediately in liquid nitrogen.

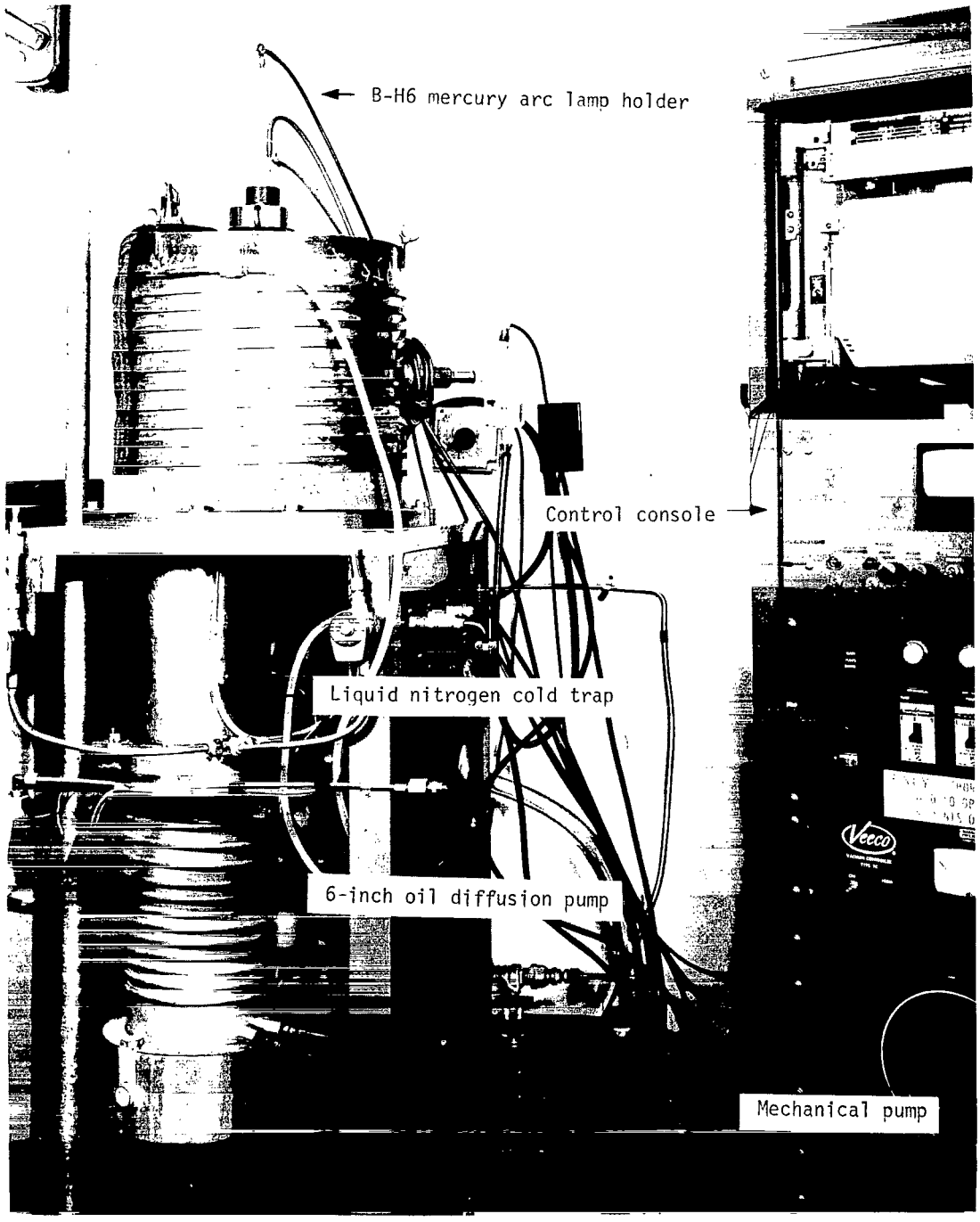

(a) Vacuum system. L-65-4842.1

Figure 1.- Testing apparatus for simulation of high vacuum and solar ultraviolet radiation.

(b) Simulated solar ultraviolet apparatus. L-65-8144.1

Figure 1.- Concluded.

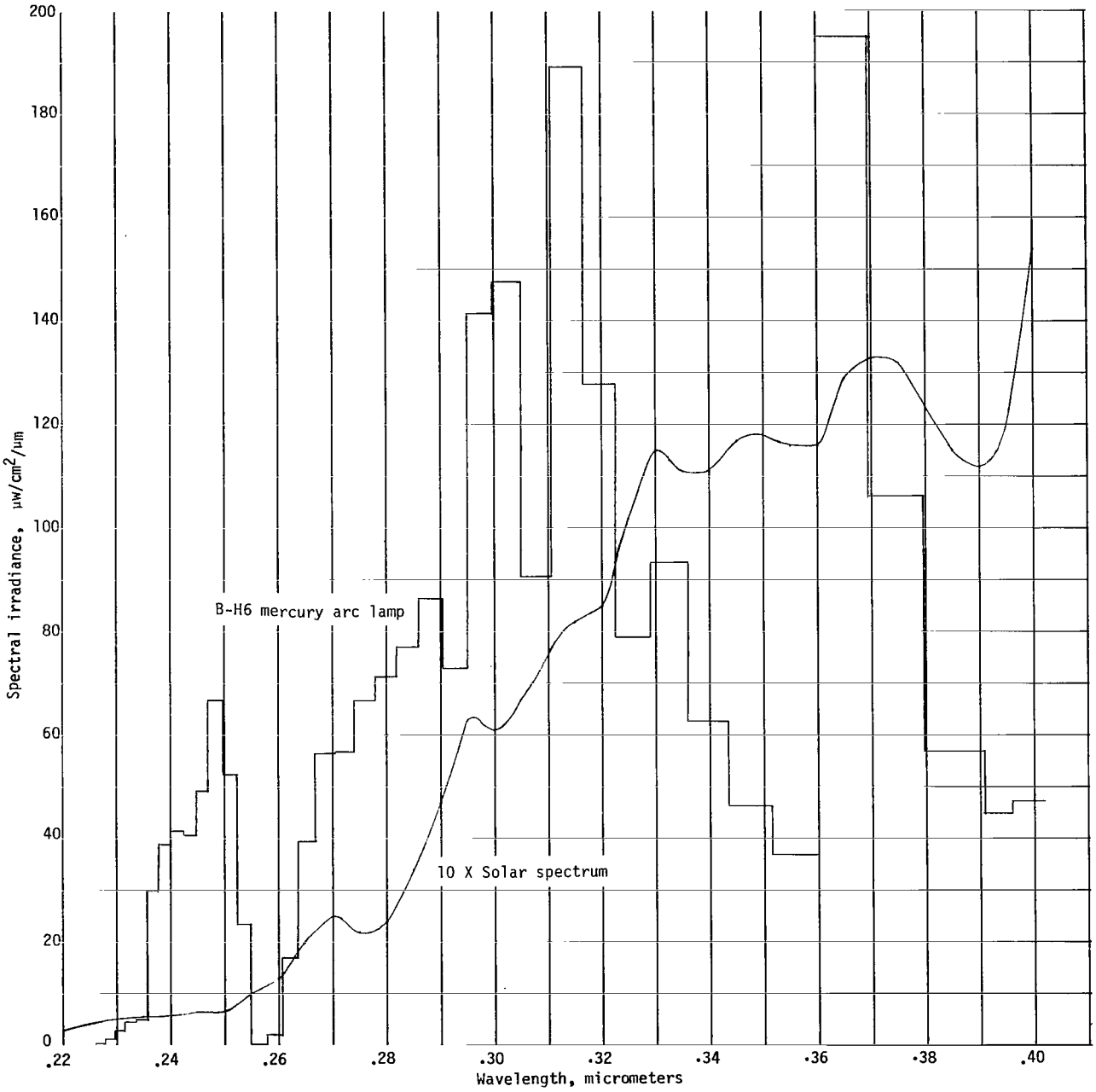

Figure 2.- Comparison of the near ultraviolet spectrum of the B-H6 mercury arc lamp and the solar spectrum.

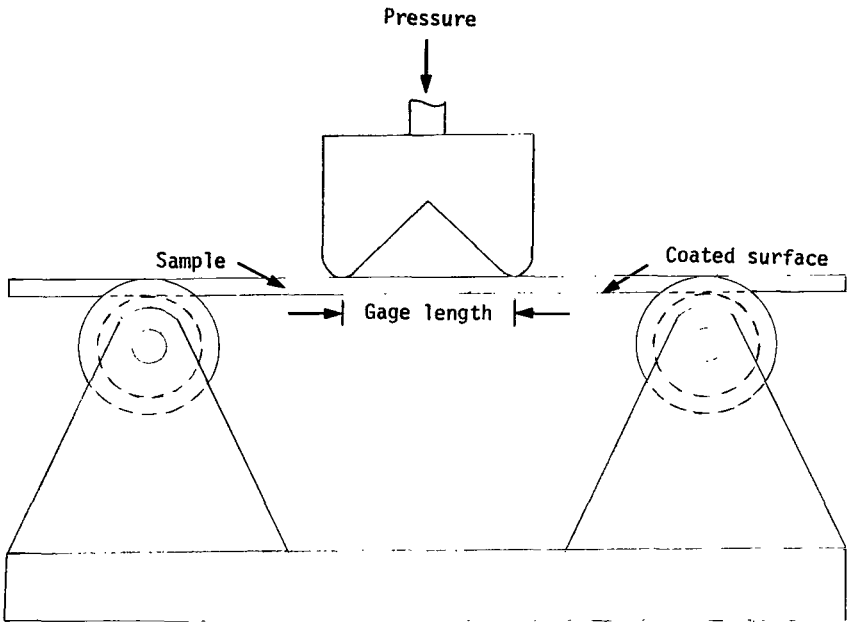

(a) Initial bend.

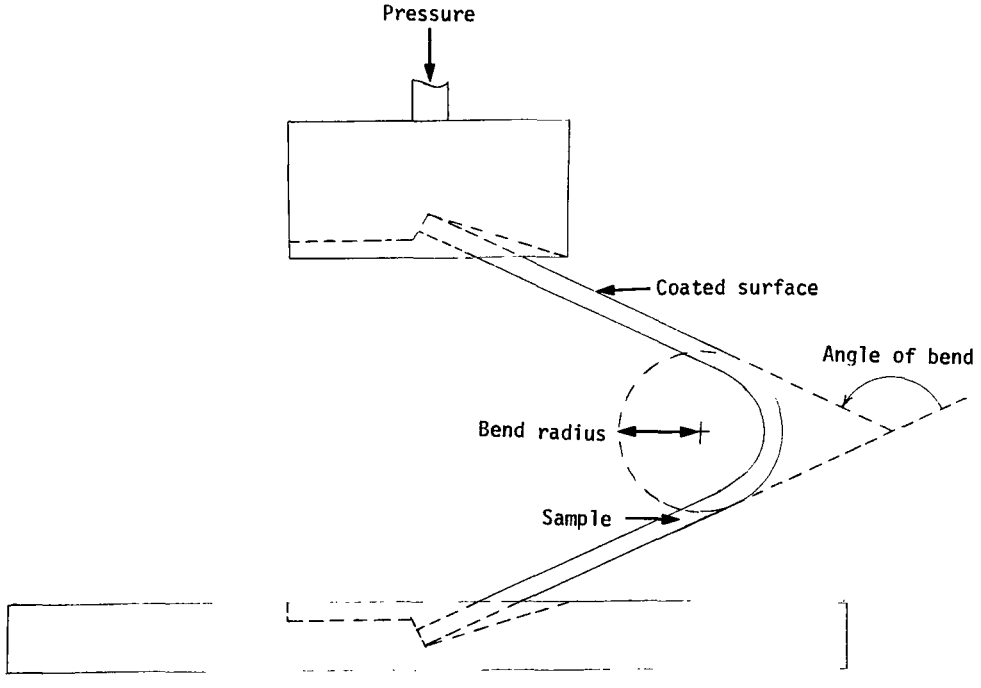

(b) Final bend.

Figure 3.- Sketch of ASTM bend test apparatus, illustrating initial bend and final bend.

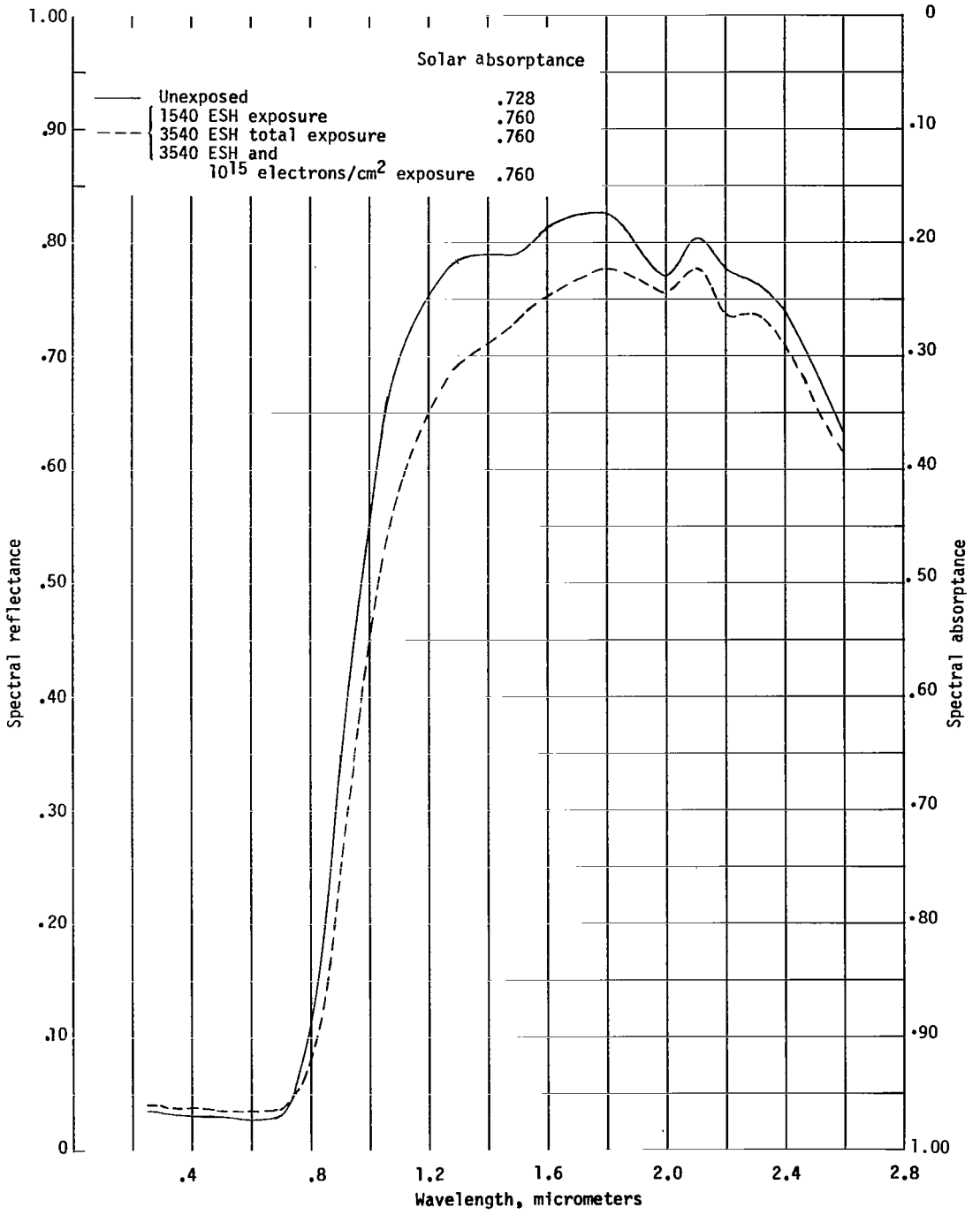

(a) Bi_2S_3 dyed anodized aluminum.

Figure 4.- Variation of spectral reflectance with wavelength prior to and after exposure to a simulated space environment.

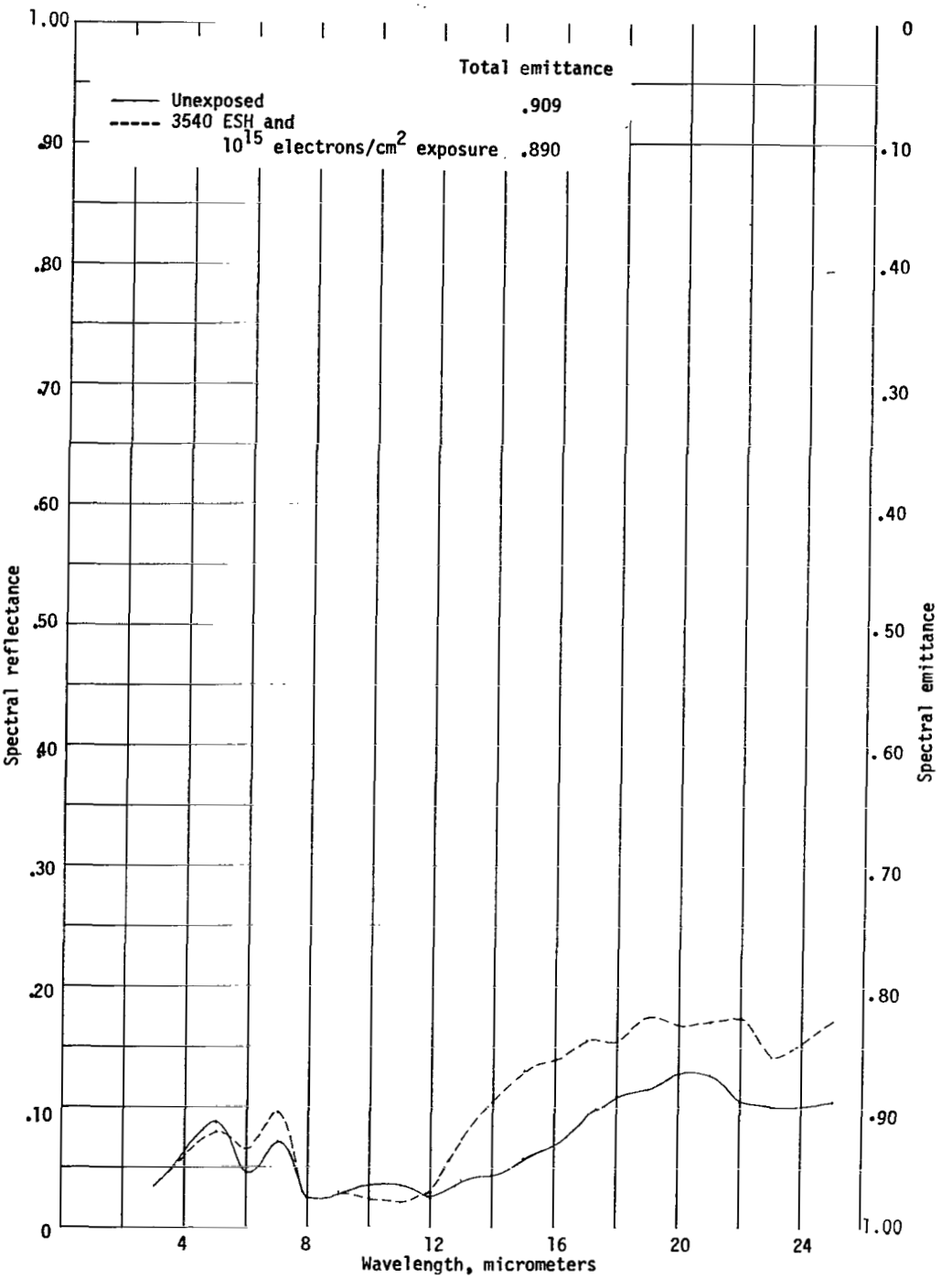

(a) Concluded.

Figure 4.- Continued.

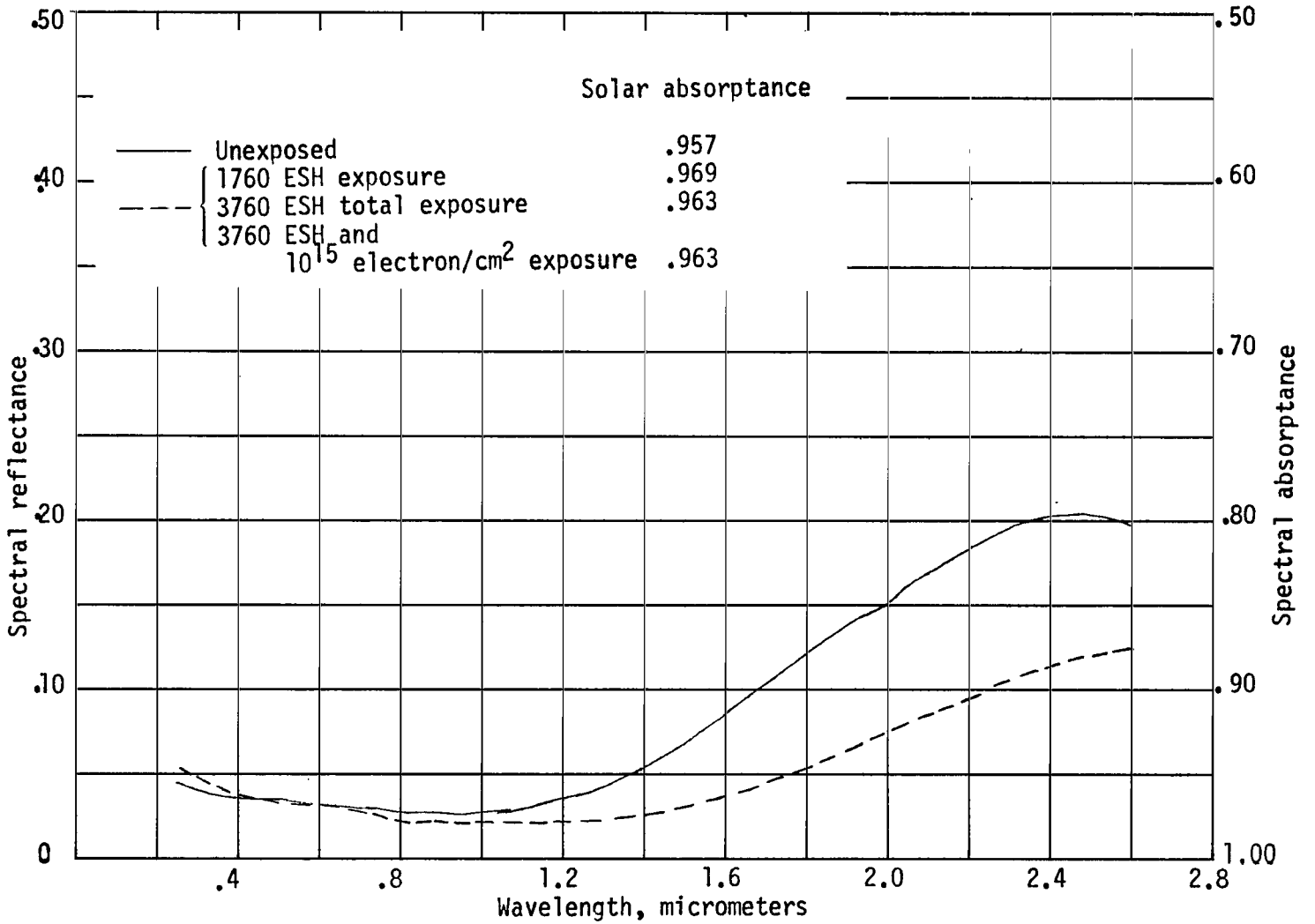

(b) CoS dyed anodized aluminum.

Figure 4.- Continued.

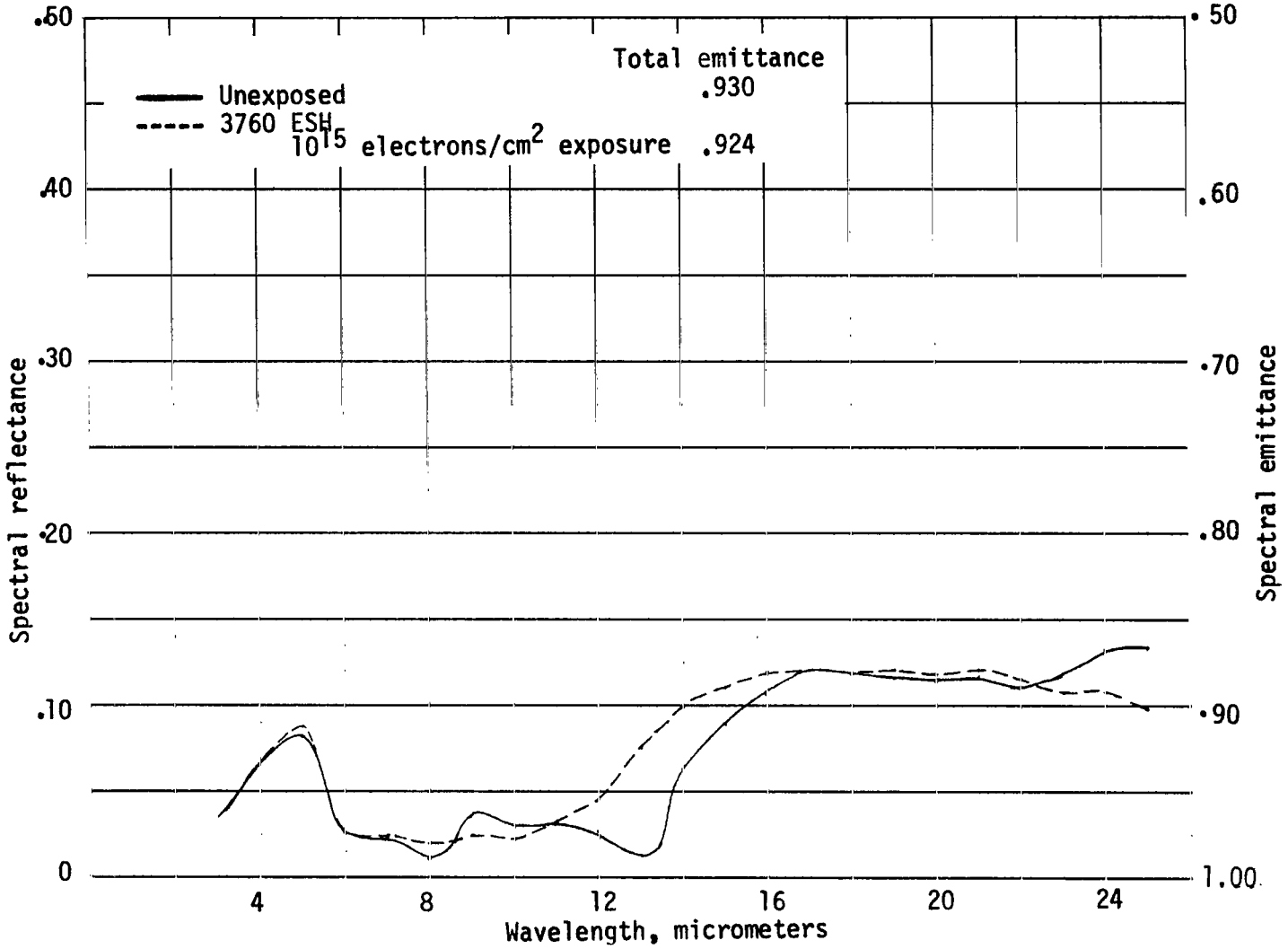

(b) Concluded.

Figure 4.- Continued.

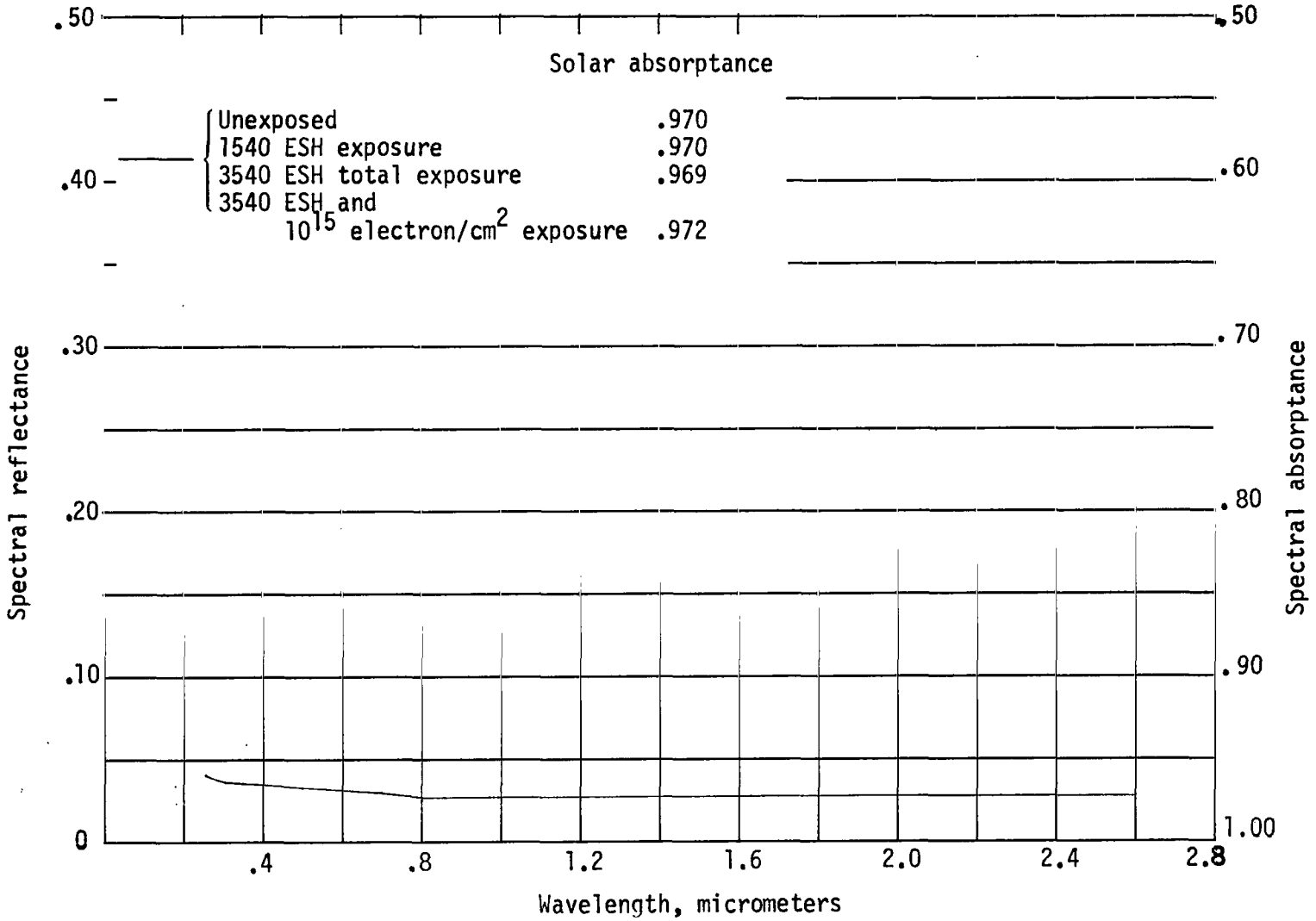

(c) NiS dyed anodized aluminum.

Figure 4.- Continued.

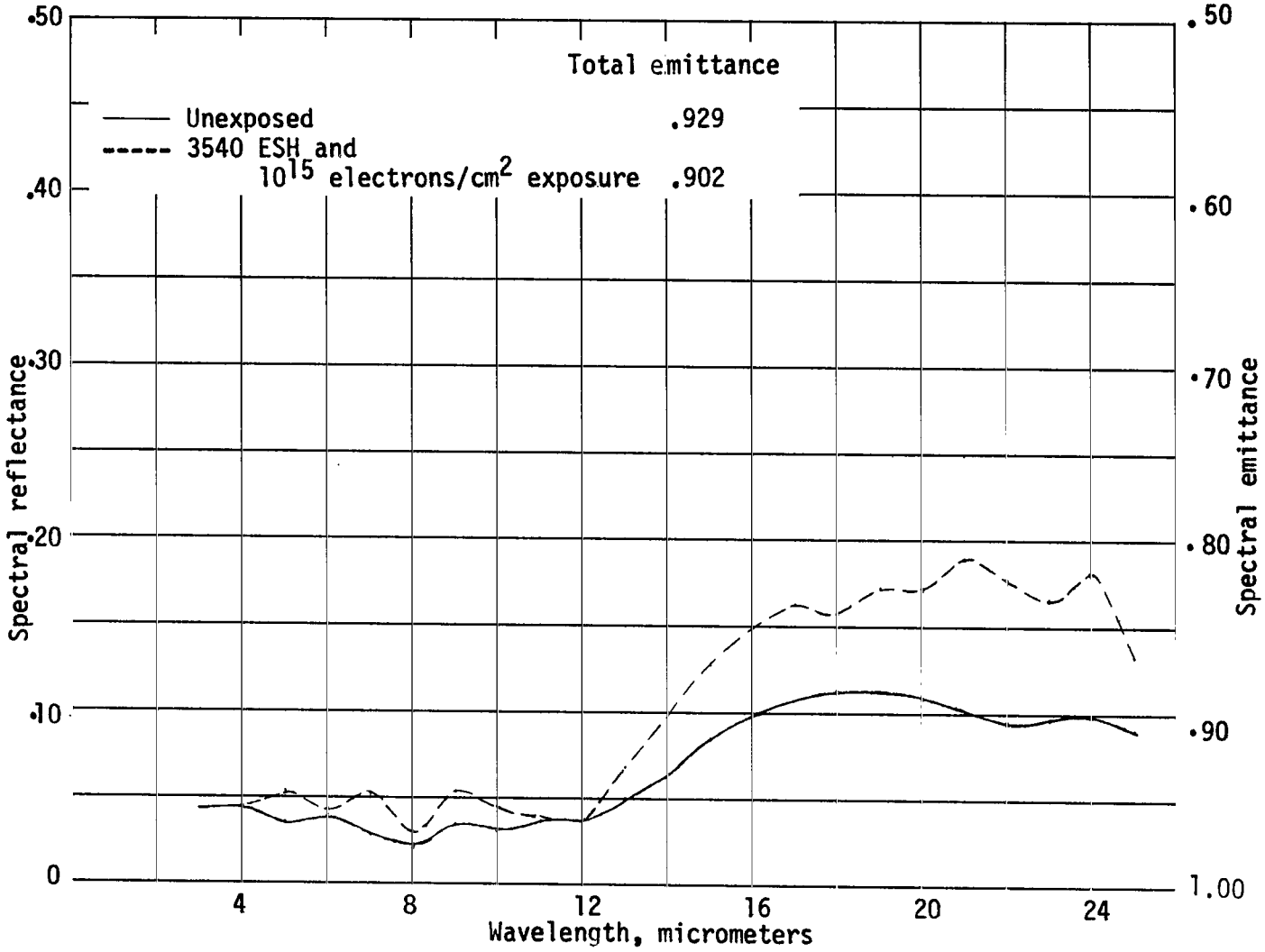

(c) Concluded.

Figure 4.- Continued.

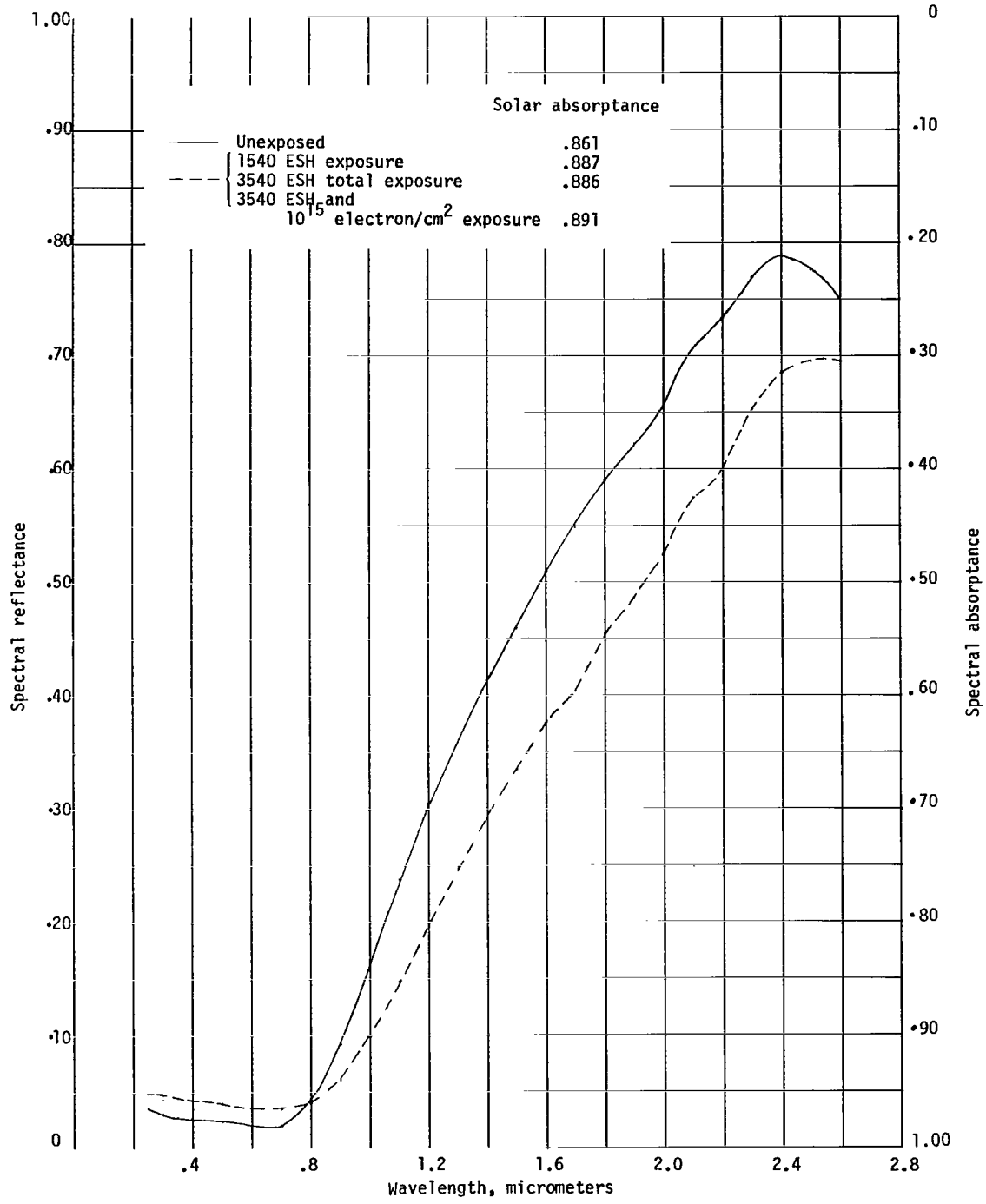

(d) PbS dyed anodized aluminum.

Figure 4.- Continued.

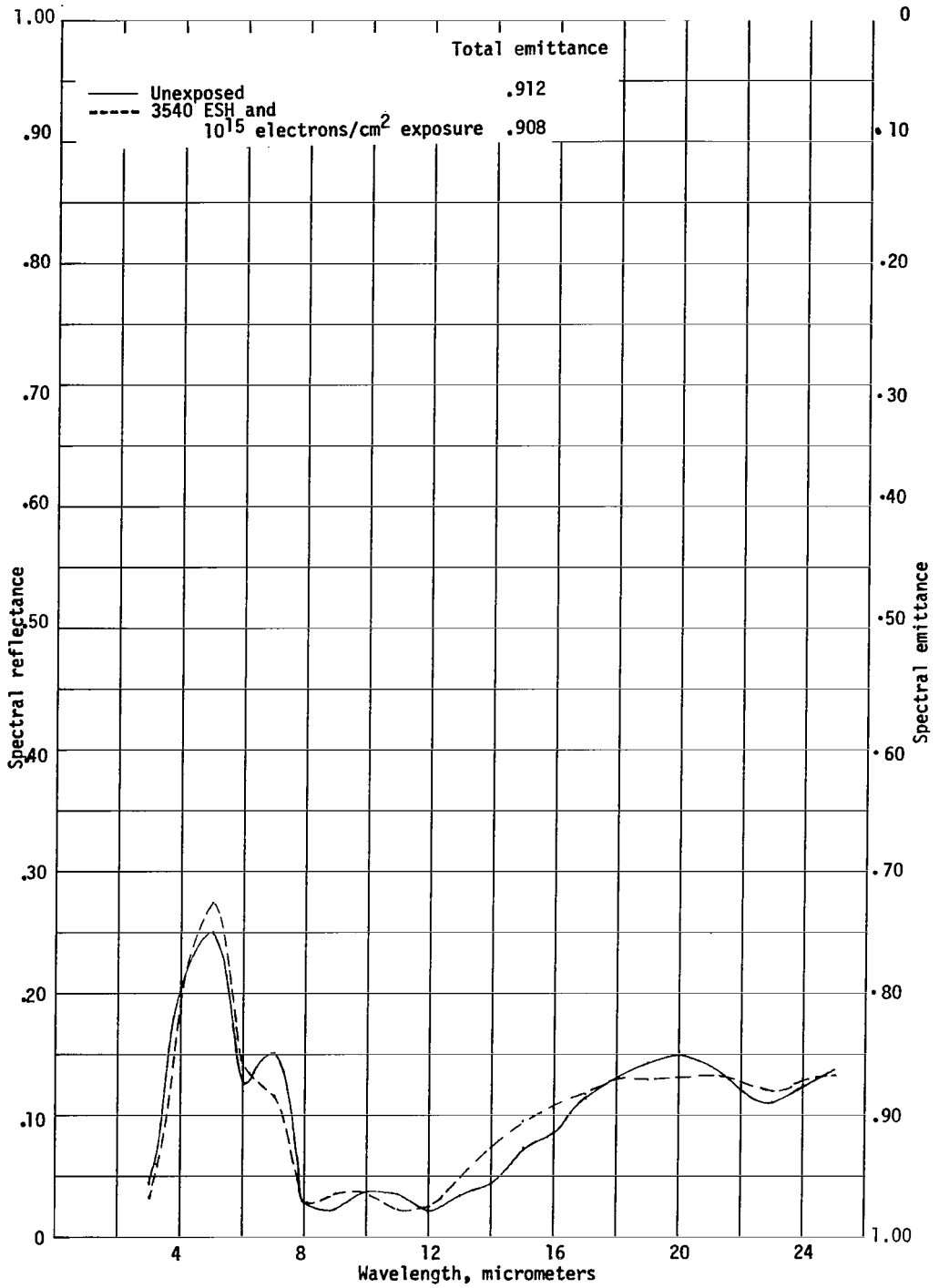

(d) Concluded.

Figure 4.- Continued.

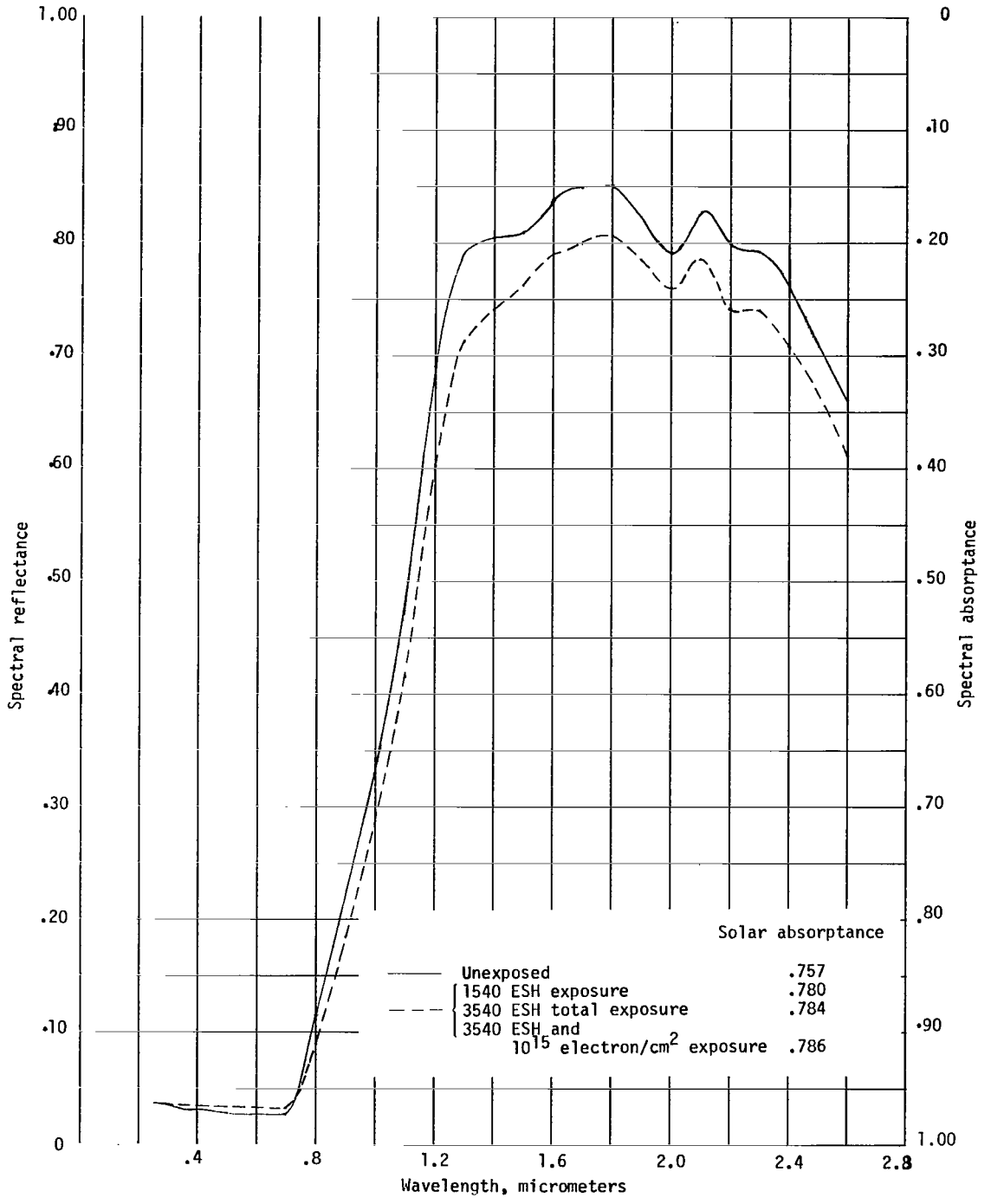

(e) Sandoz Black BK dyed anodized aluminum.

Figure 4.- Continued.

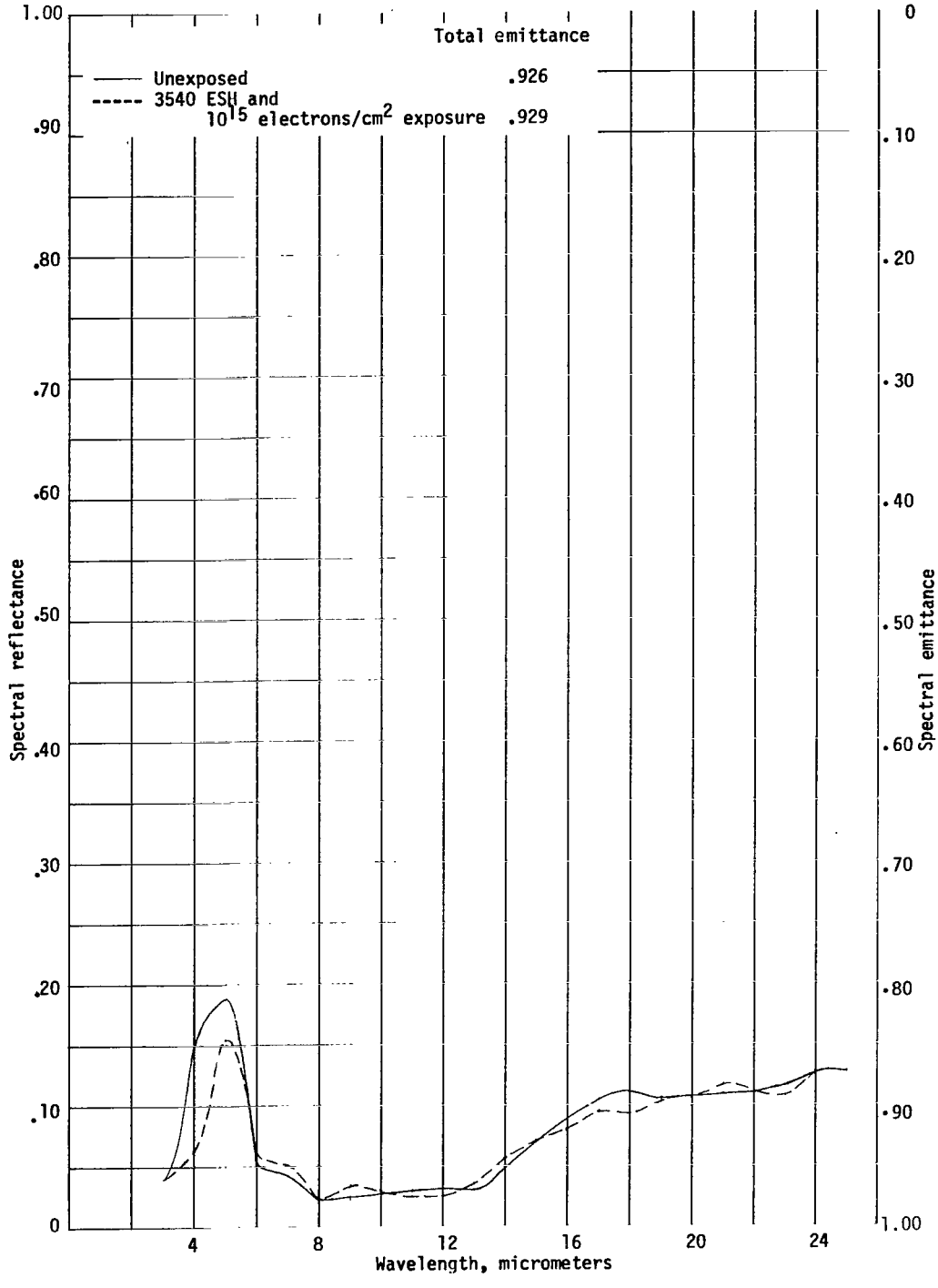

(e) Concluded.

Figure 4.- Continued.

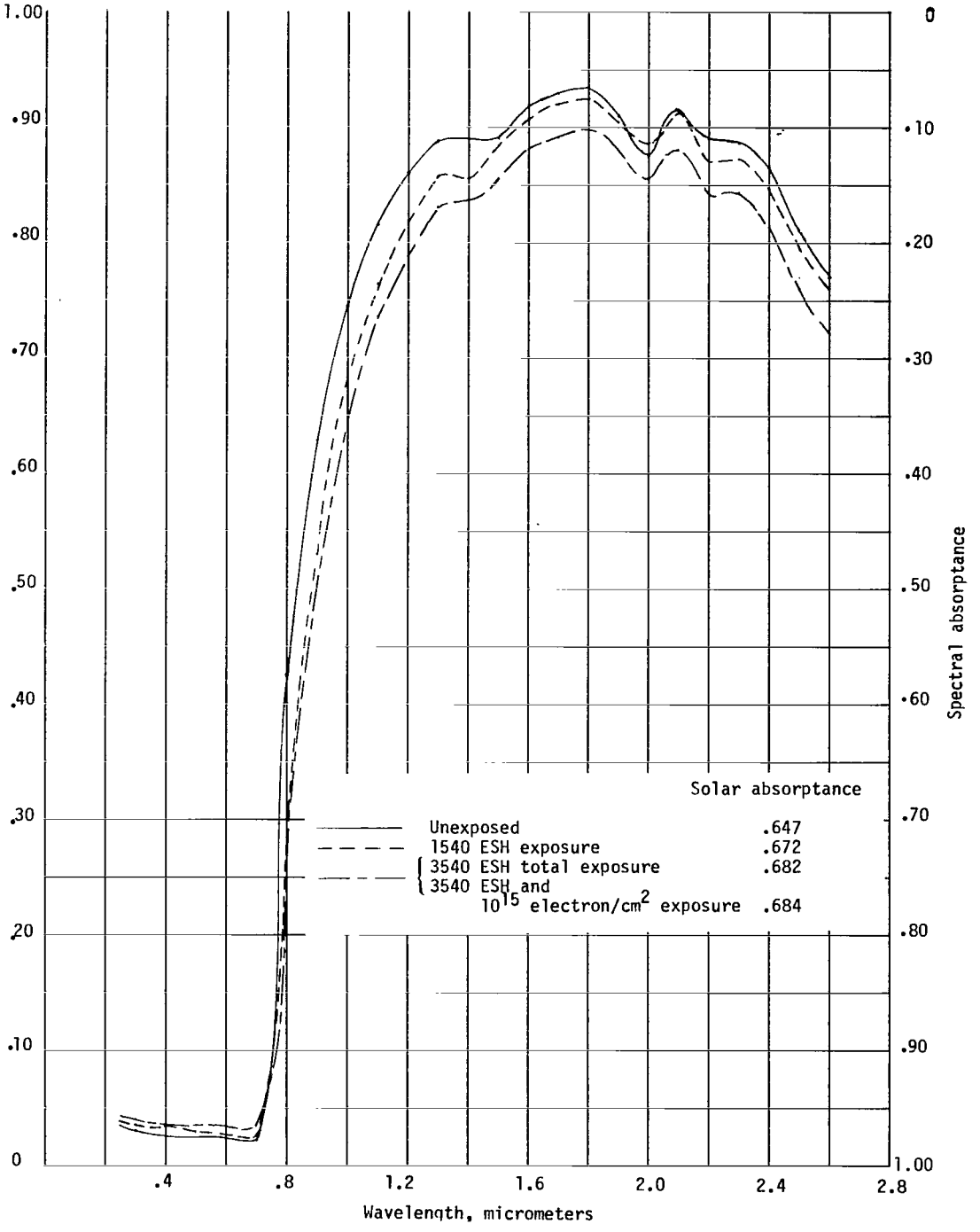

(f) Sandoz Black OA dyed anodized aluminum.

Figure 4.- Continued.

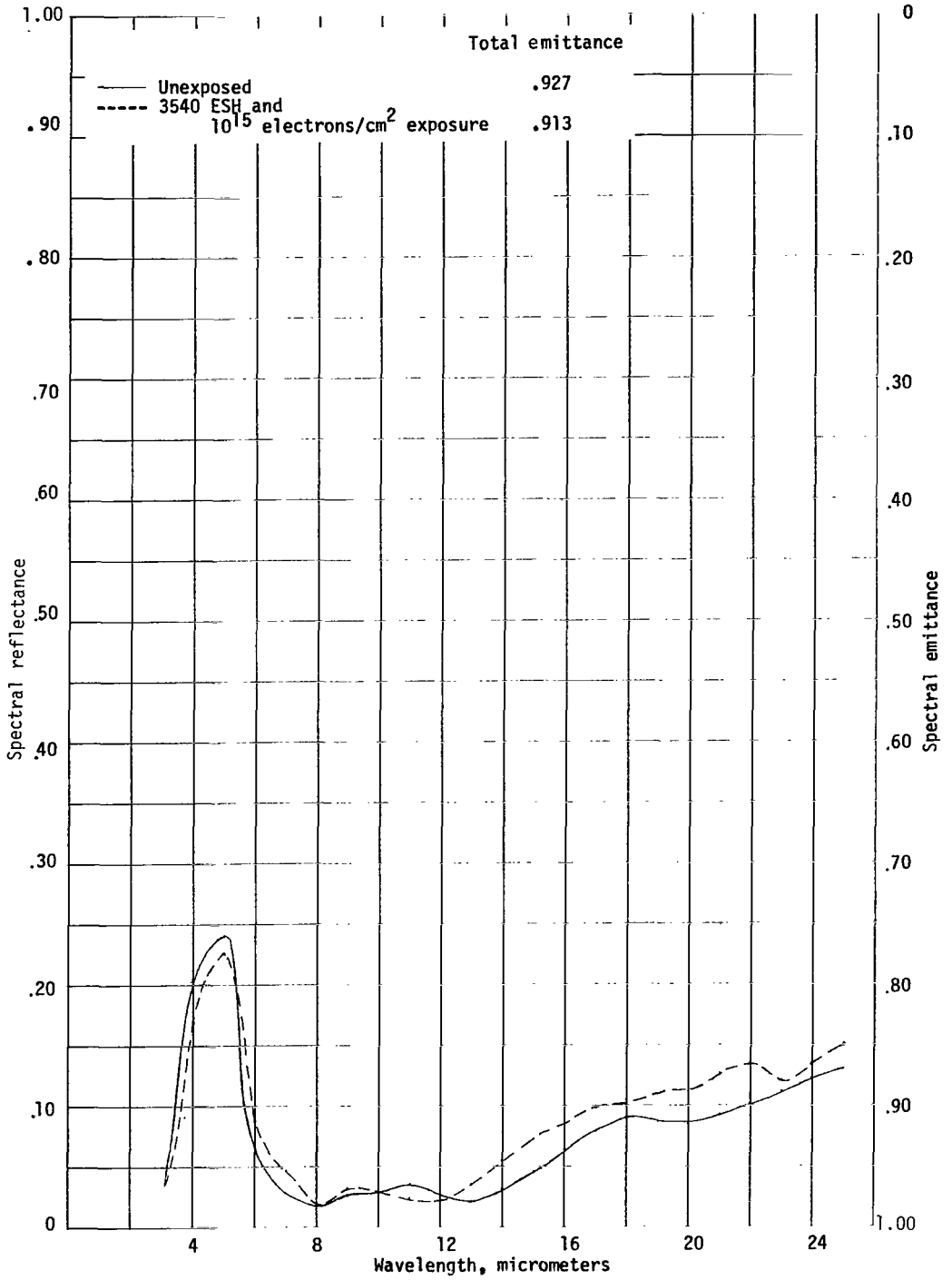

(f) Concluded.

Figure 4.- Continued.

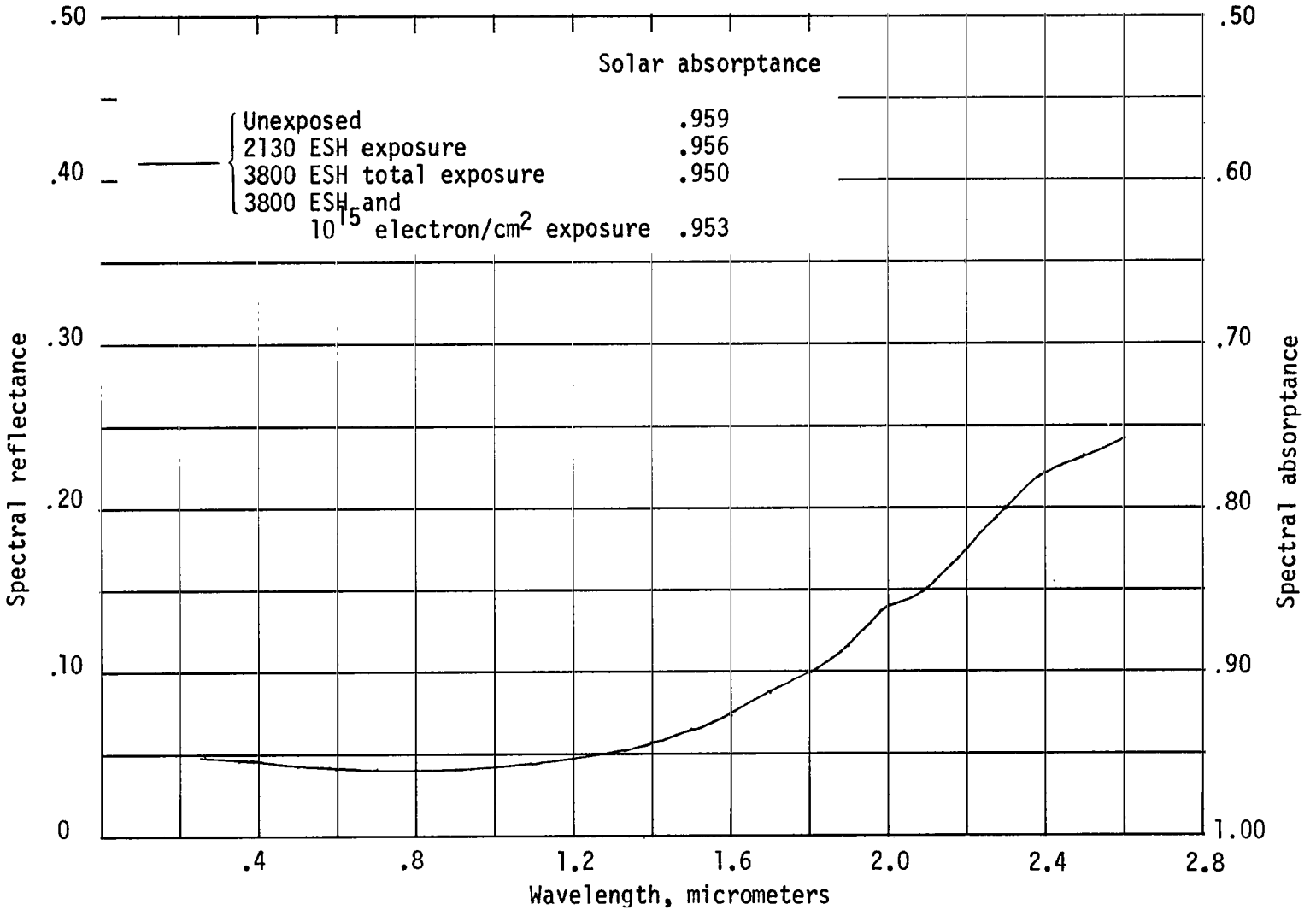

(g) Black nickel plate on aluminum.

Figure 4.- Continued.

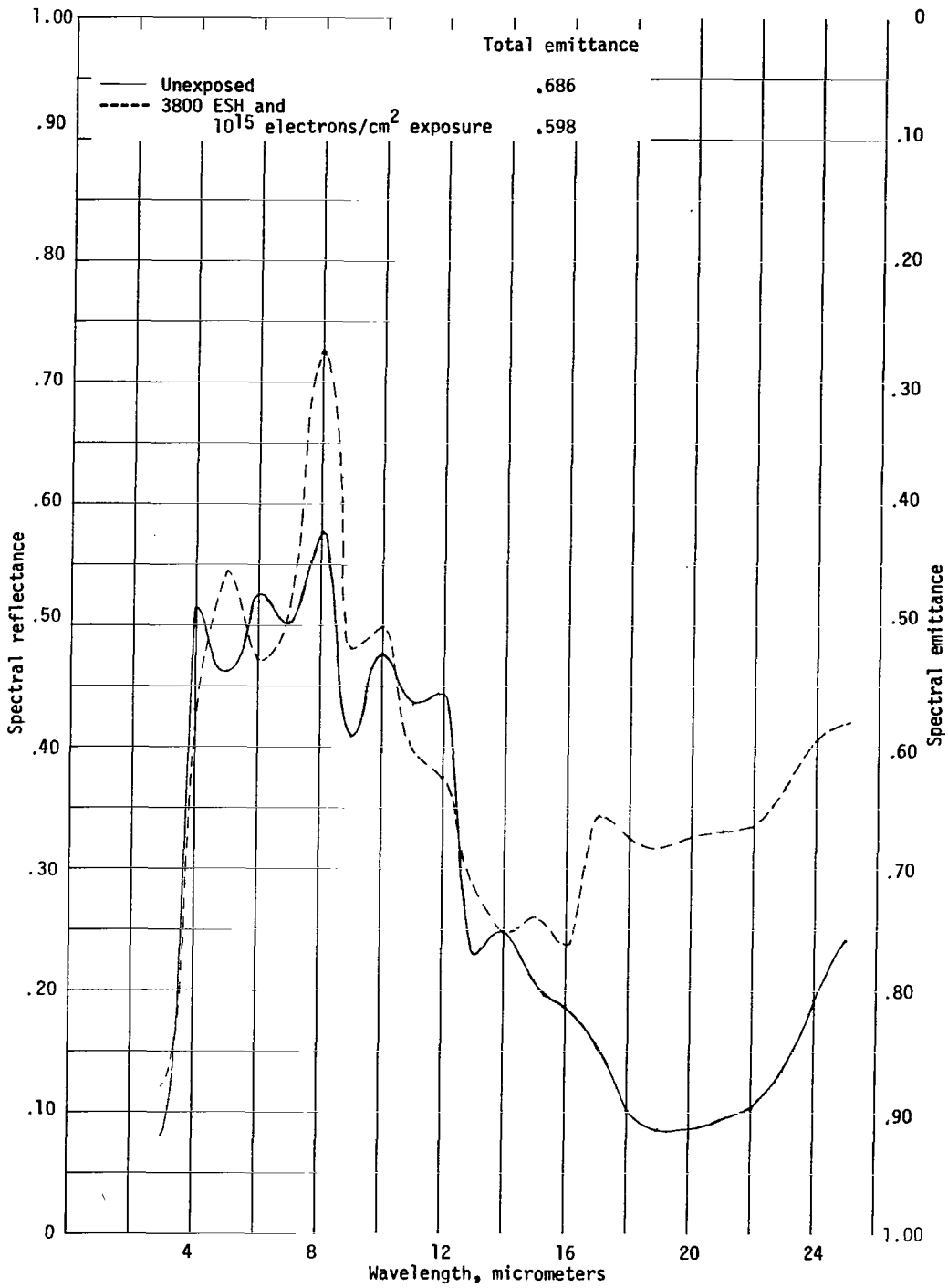

(g) Concluded.

Figure 4.- Continued.

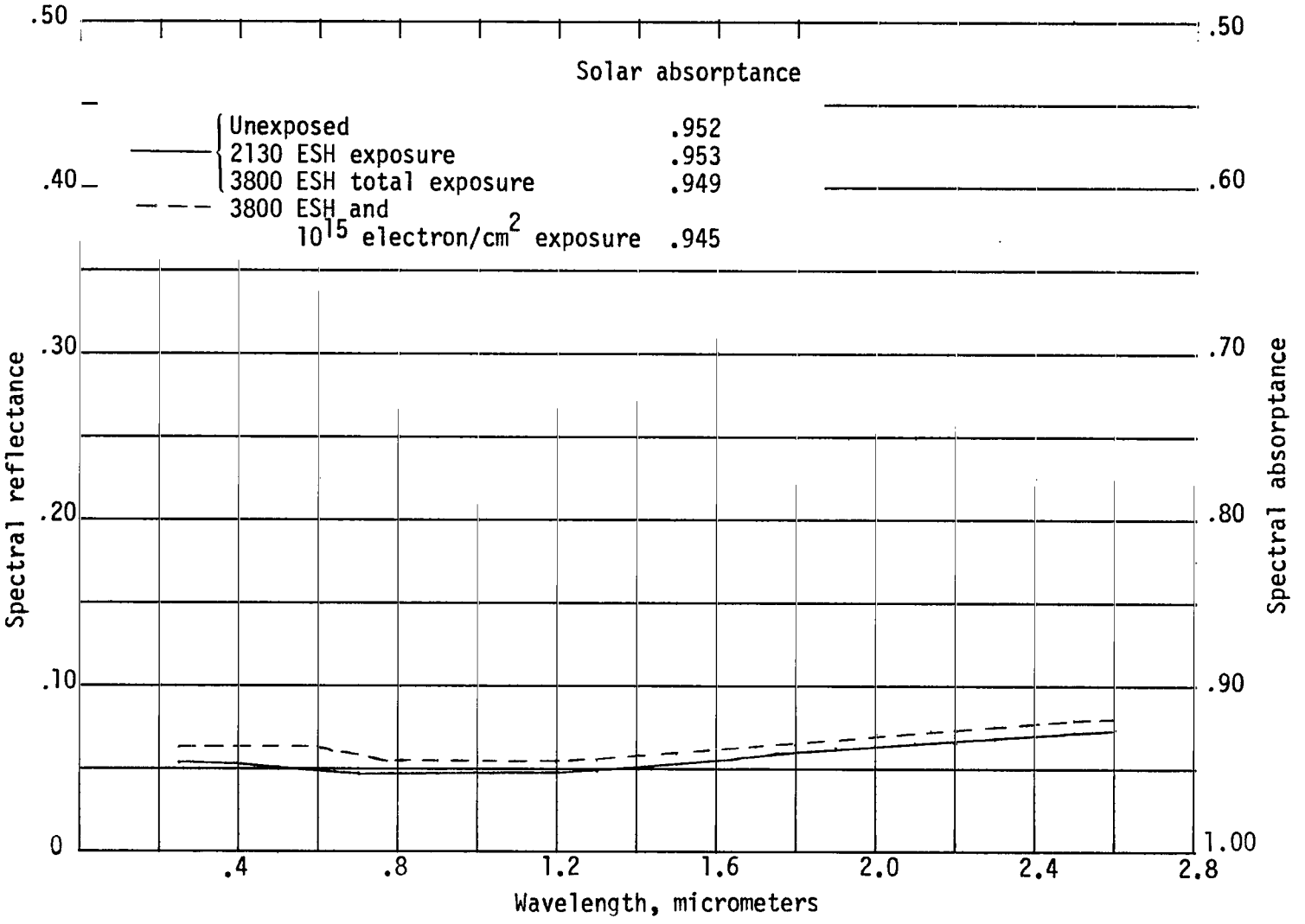

(h) Du-Lite 3-0 on grit-blasted type 3-4 stainless steel.

Figure 4.- Continued.

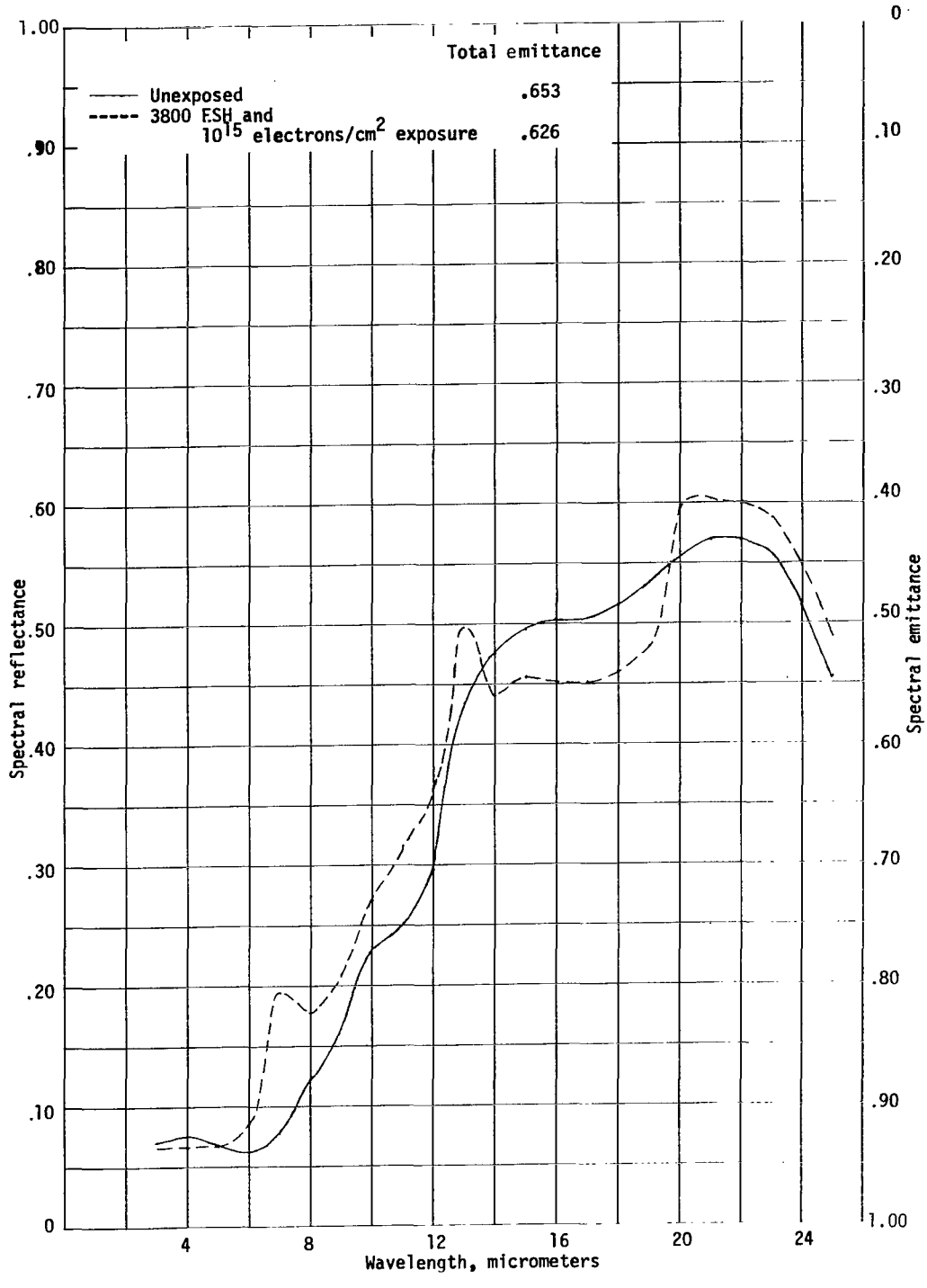

(h) Concluded.

Figure 4.- Continued.

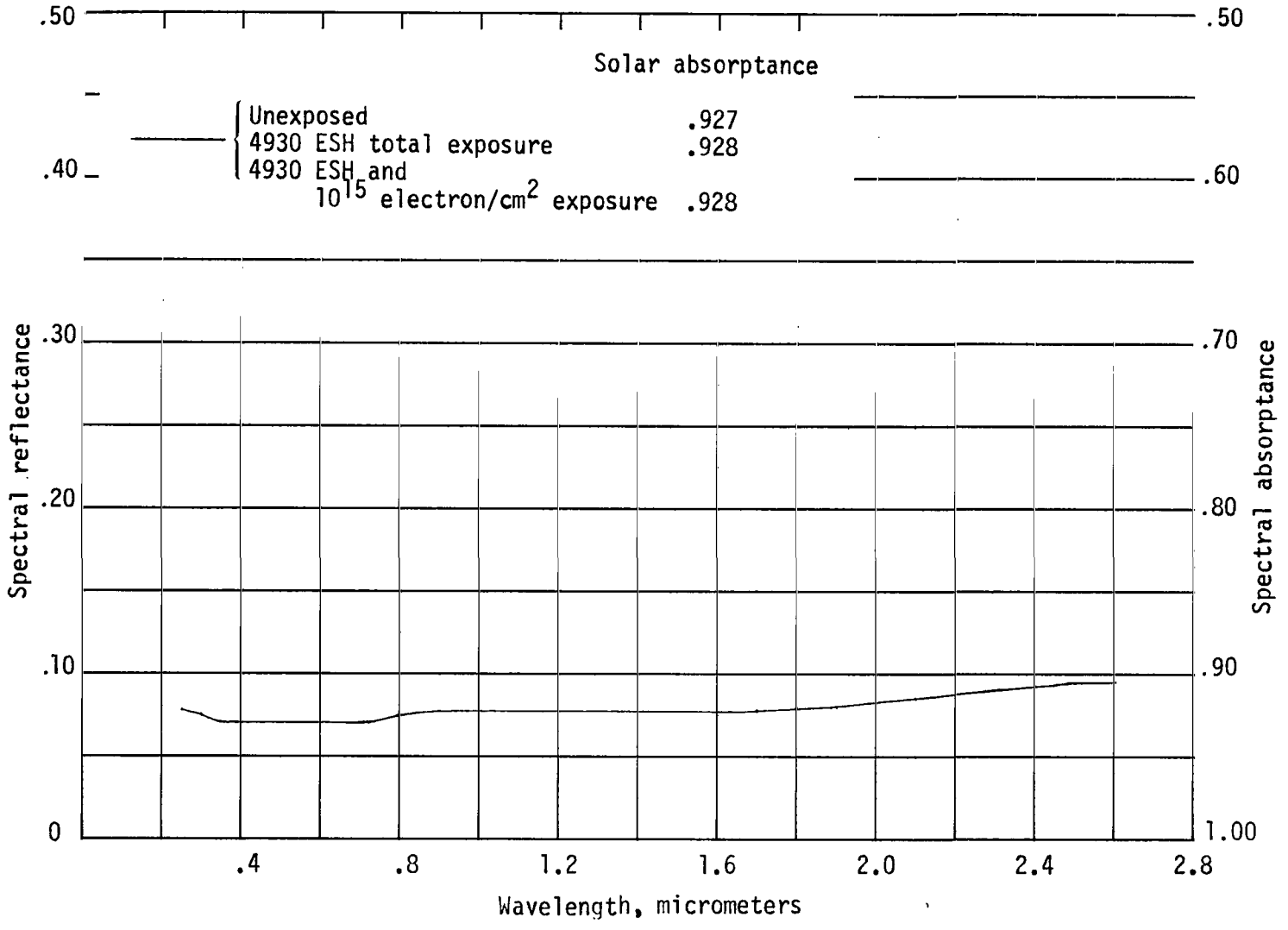

(i) Westinghouse Black on inconel.

Figure 4.- Continued.

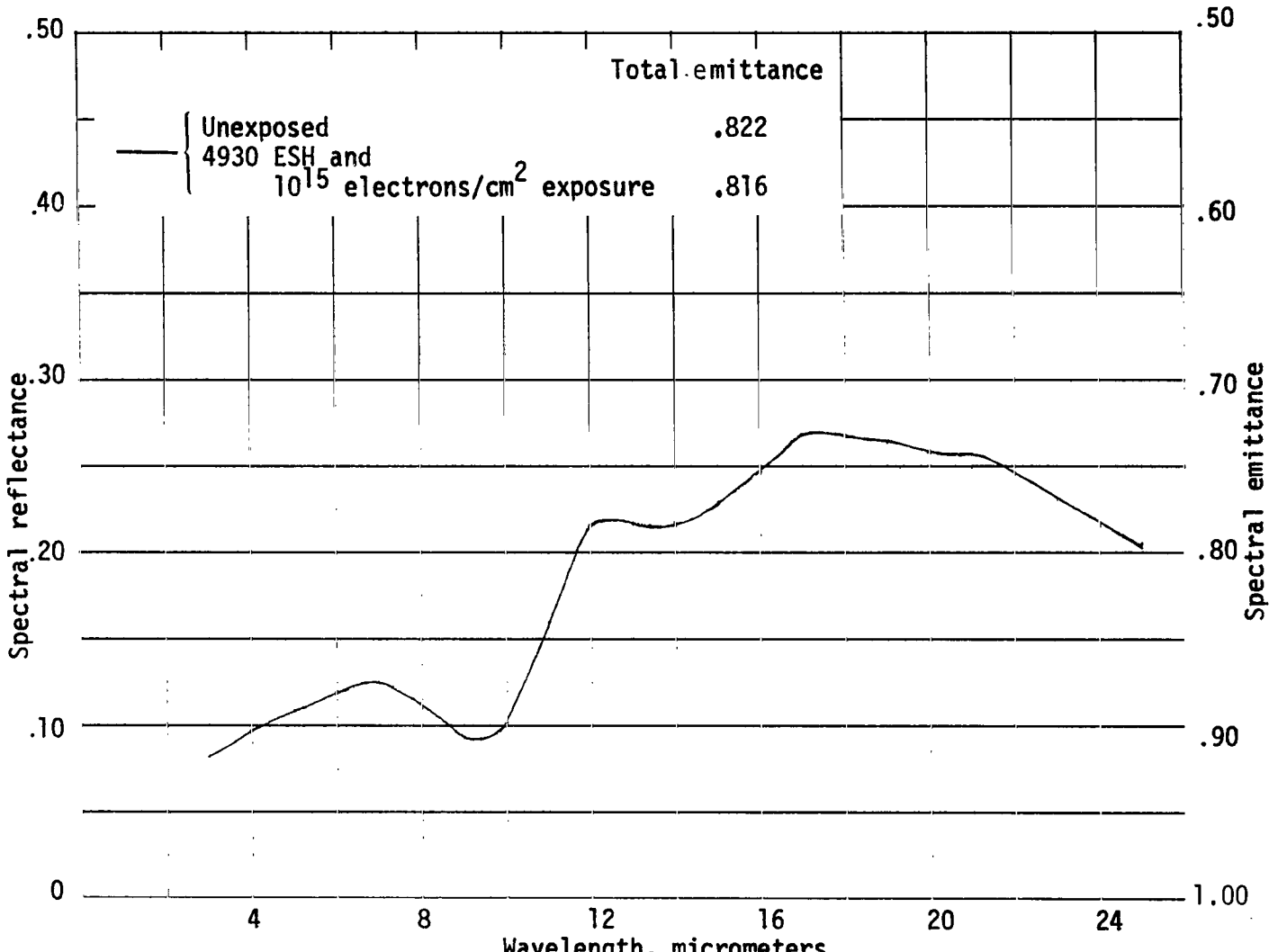

(i) Concluded.

Figure 4.- Continued.

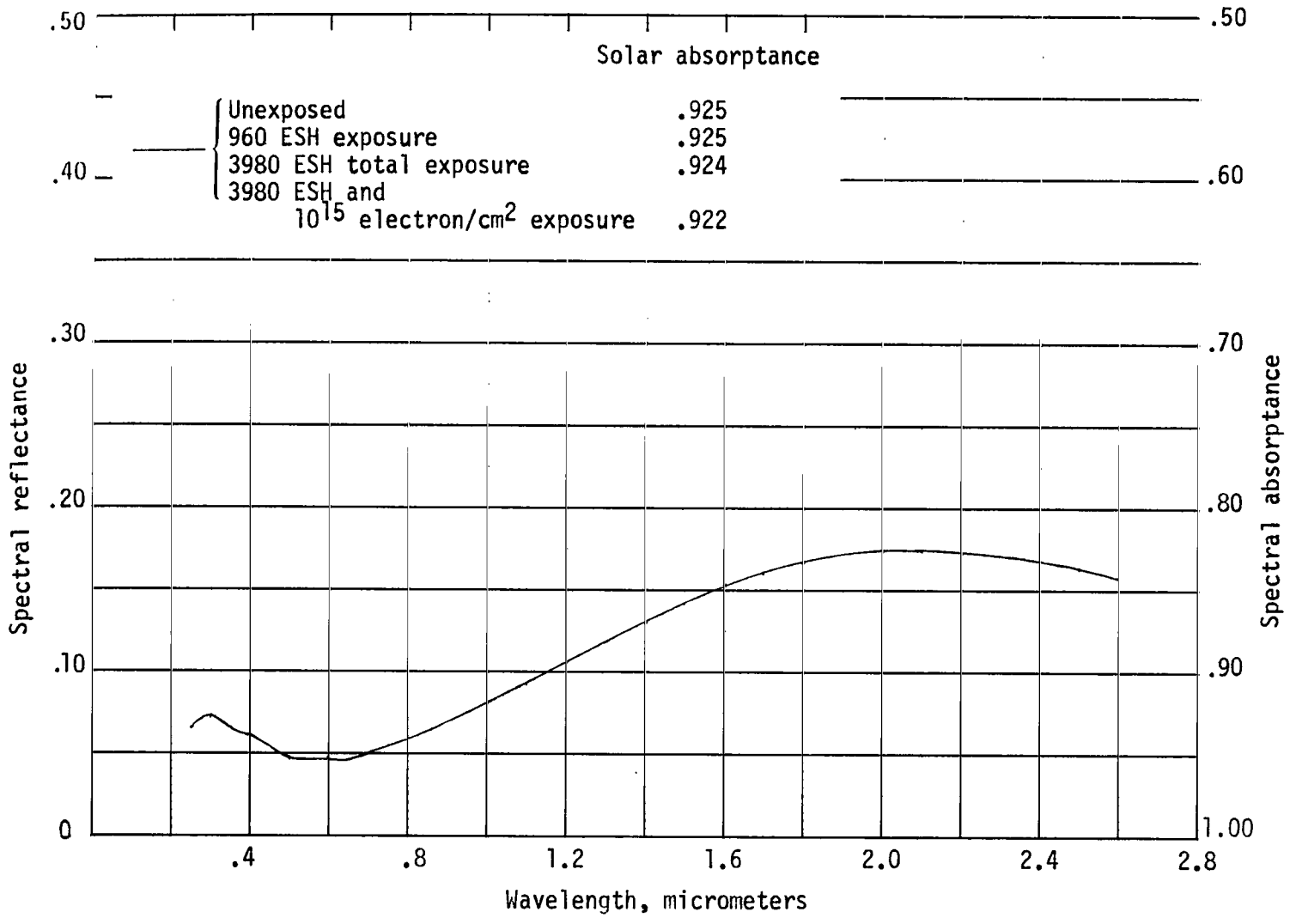

(j) Sodium dichromate blackened type 347 stainless steel.

Figure 4.- Continued.

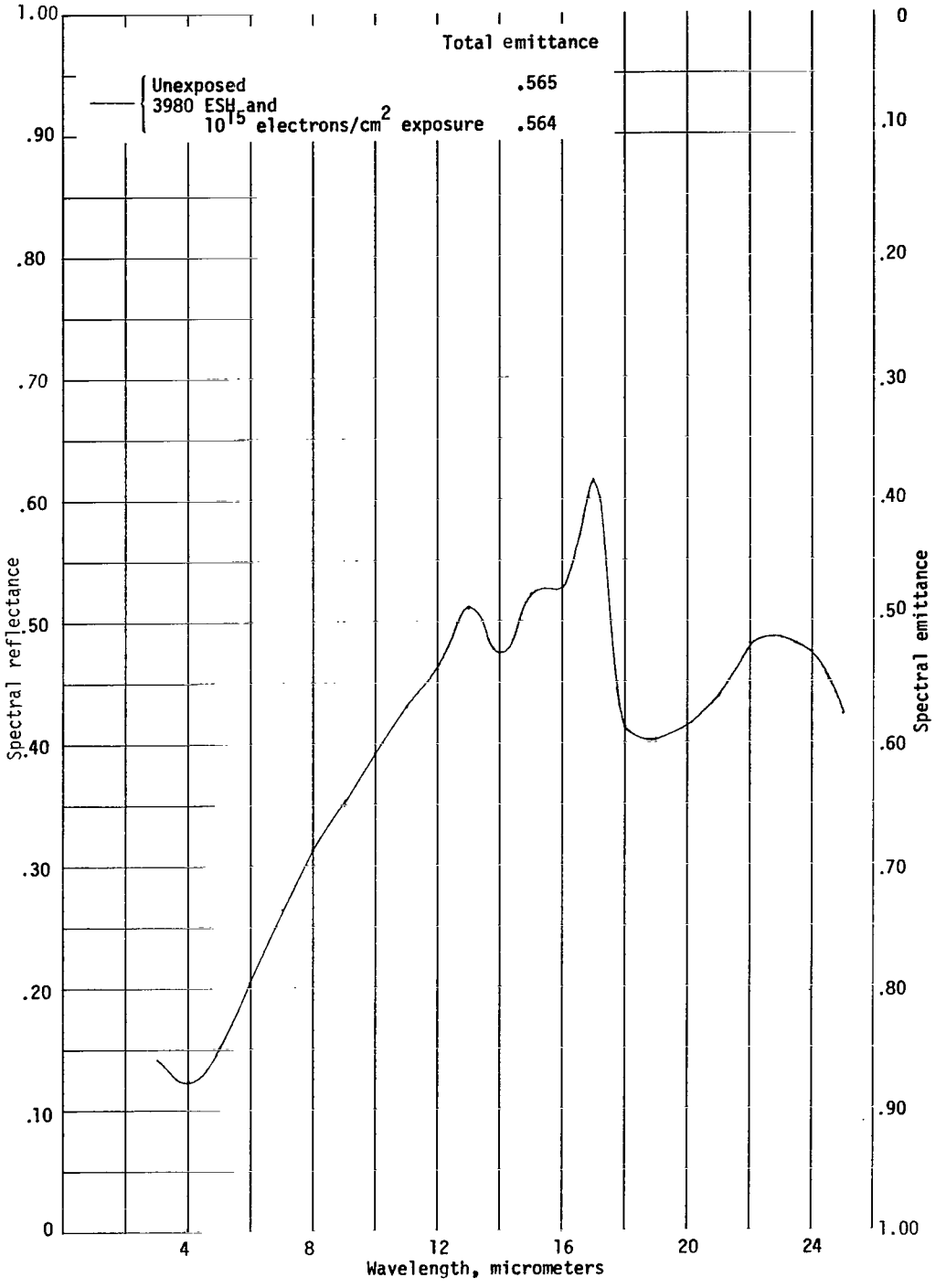

(j) Concluded.

Figure 4.- Continued.

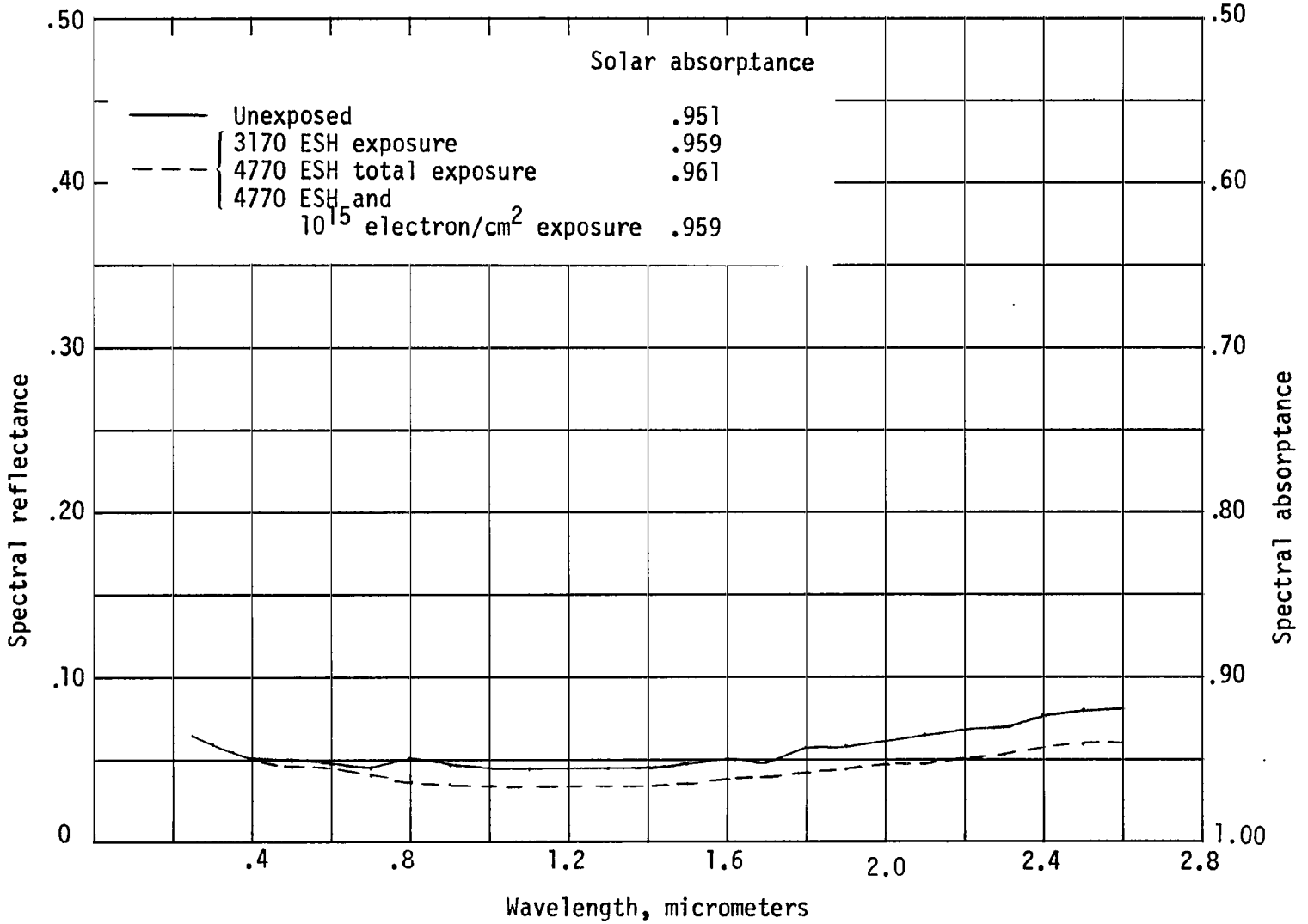

(k) Sodium dichromate blackened inconel.

Figure 4.- Continued.

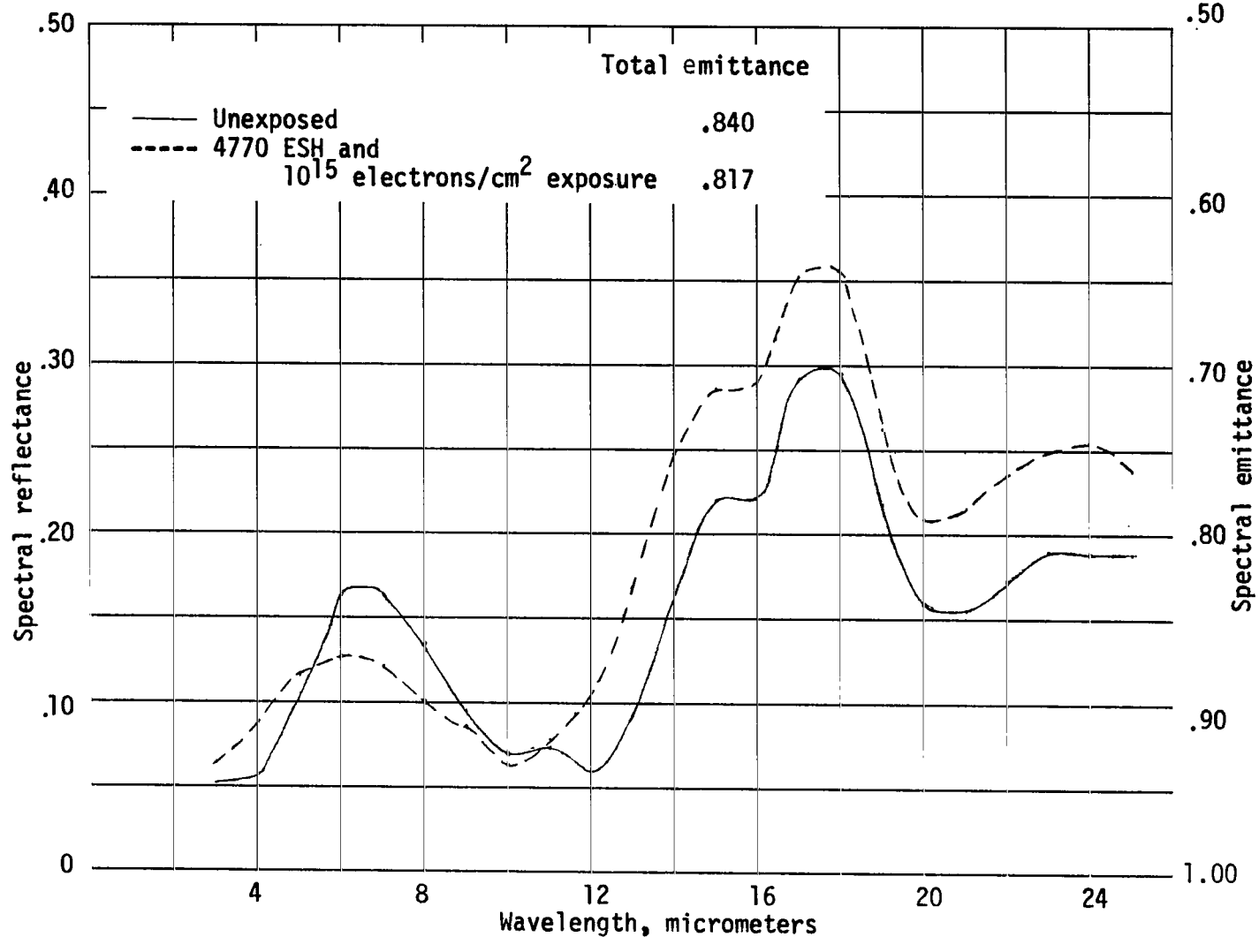

(k) Concluded.

Figure 4.- Continued.

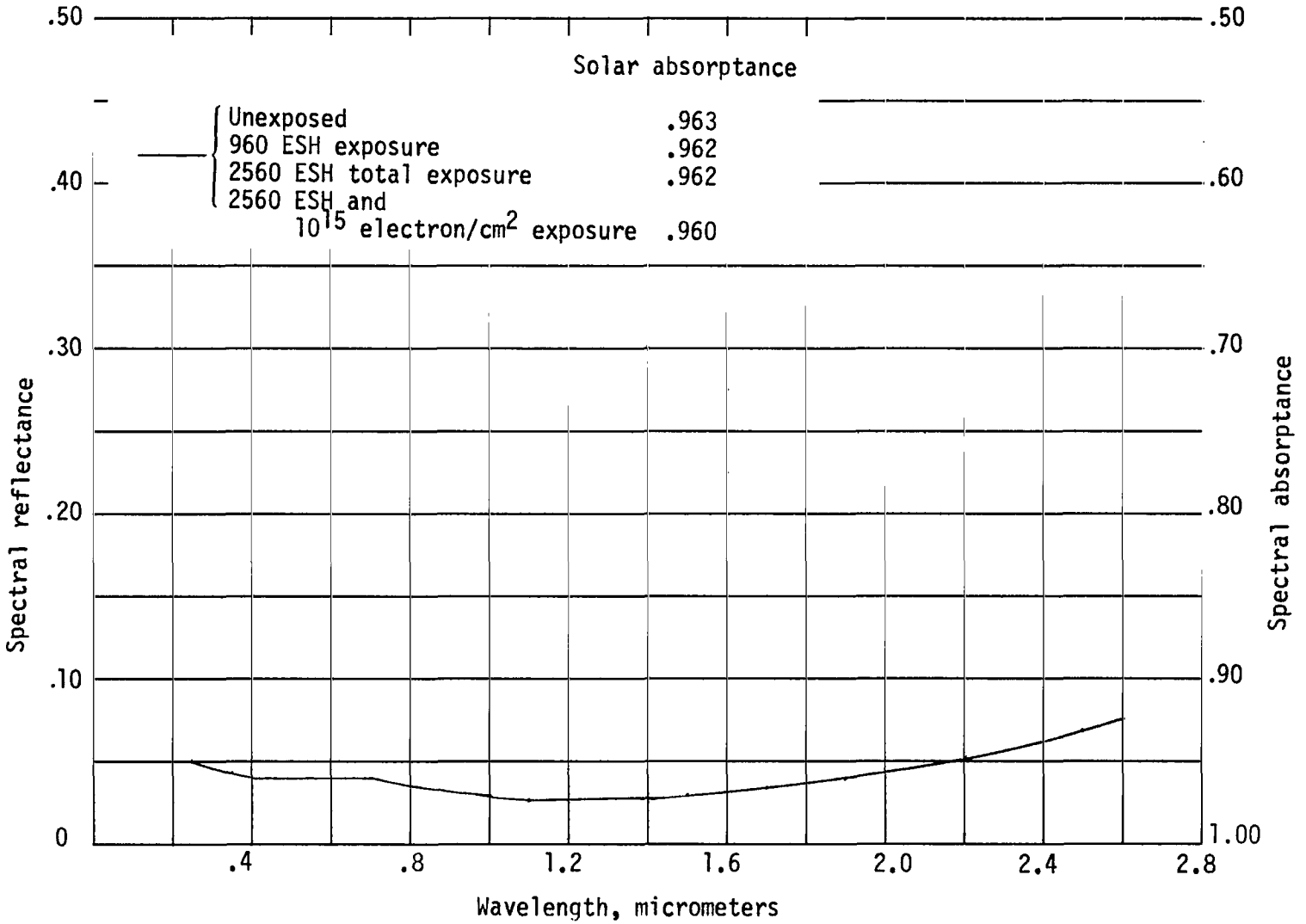

(l) Sodium dichromate blackened inconel x.

Figure 4.- Continued.

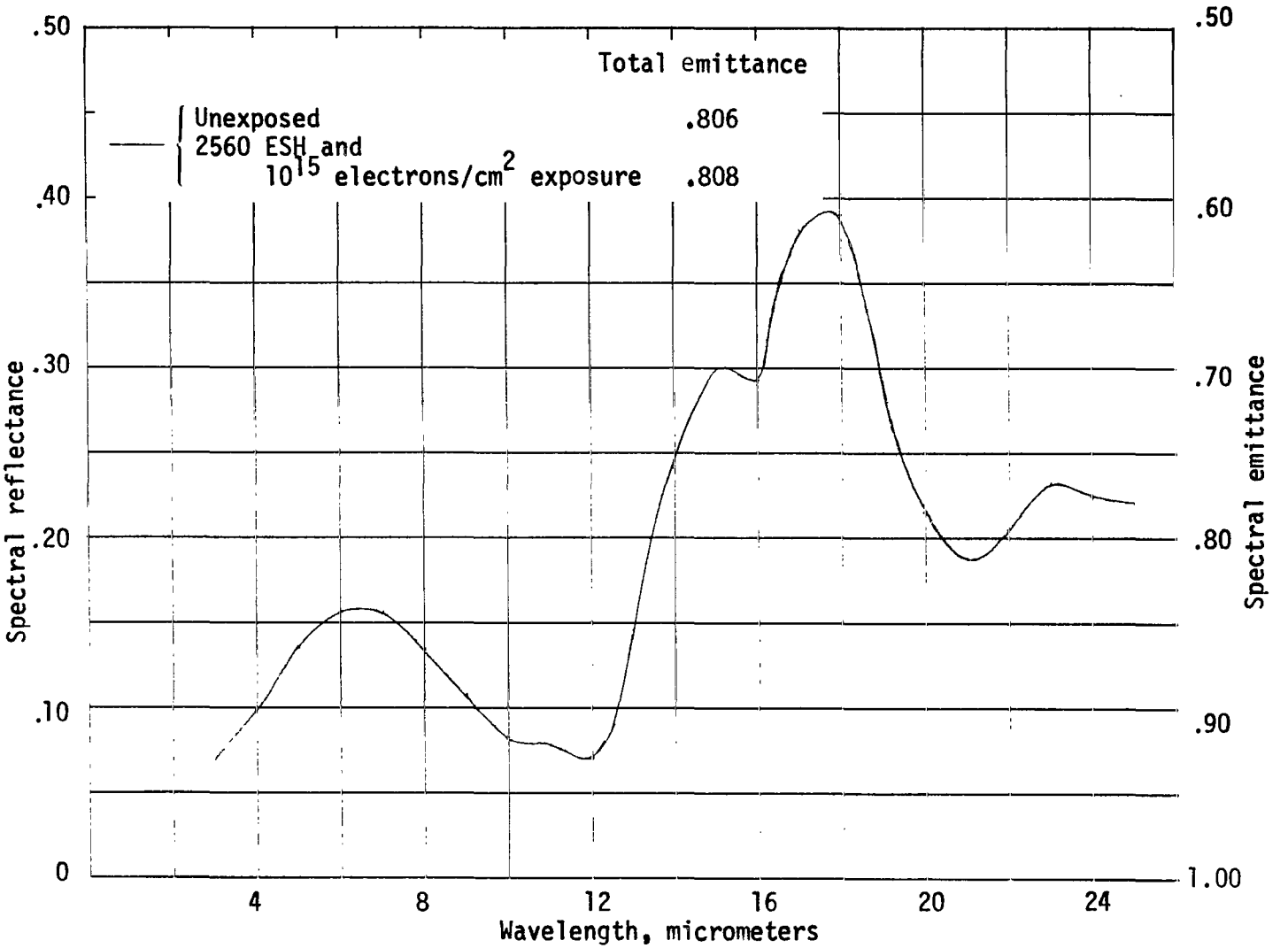

(l) Concluded.

Figure 4.- Continued.

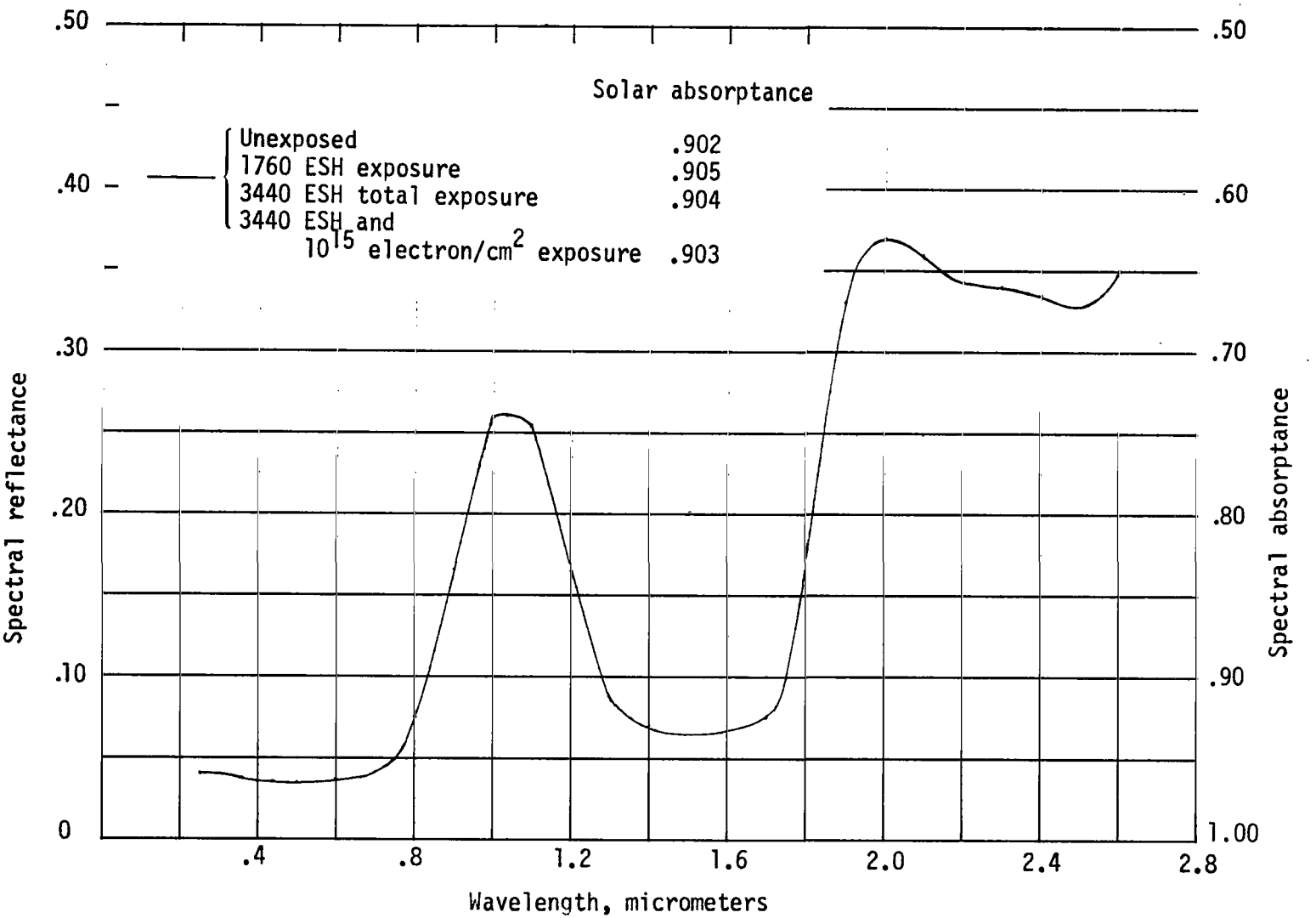

(m) Pyromark Black on aluminum.

Figure 4.- Continued.

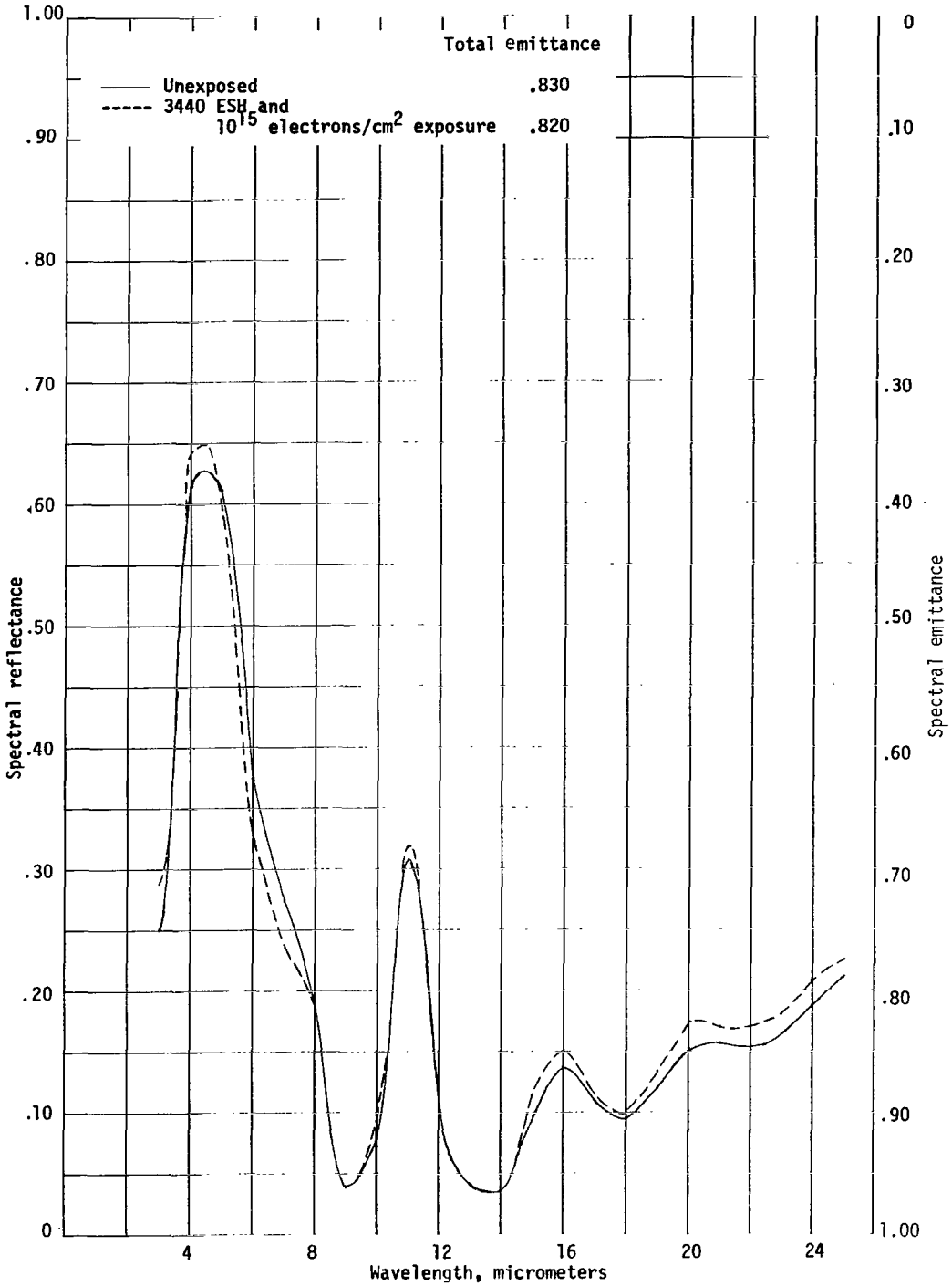

(m) Concluded.

Figure 4.- Continued.

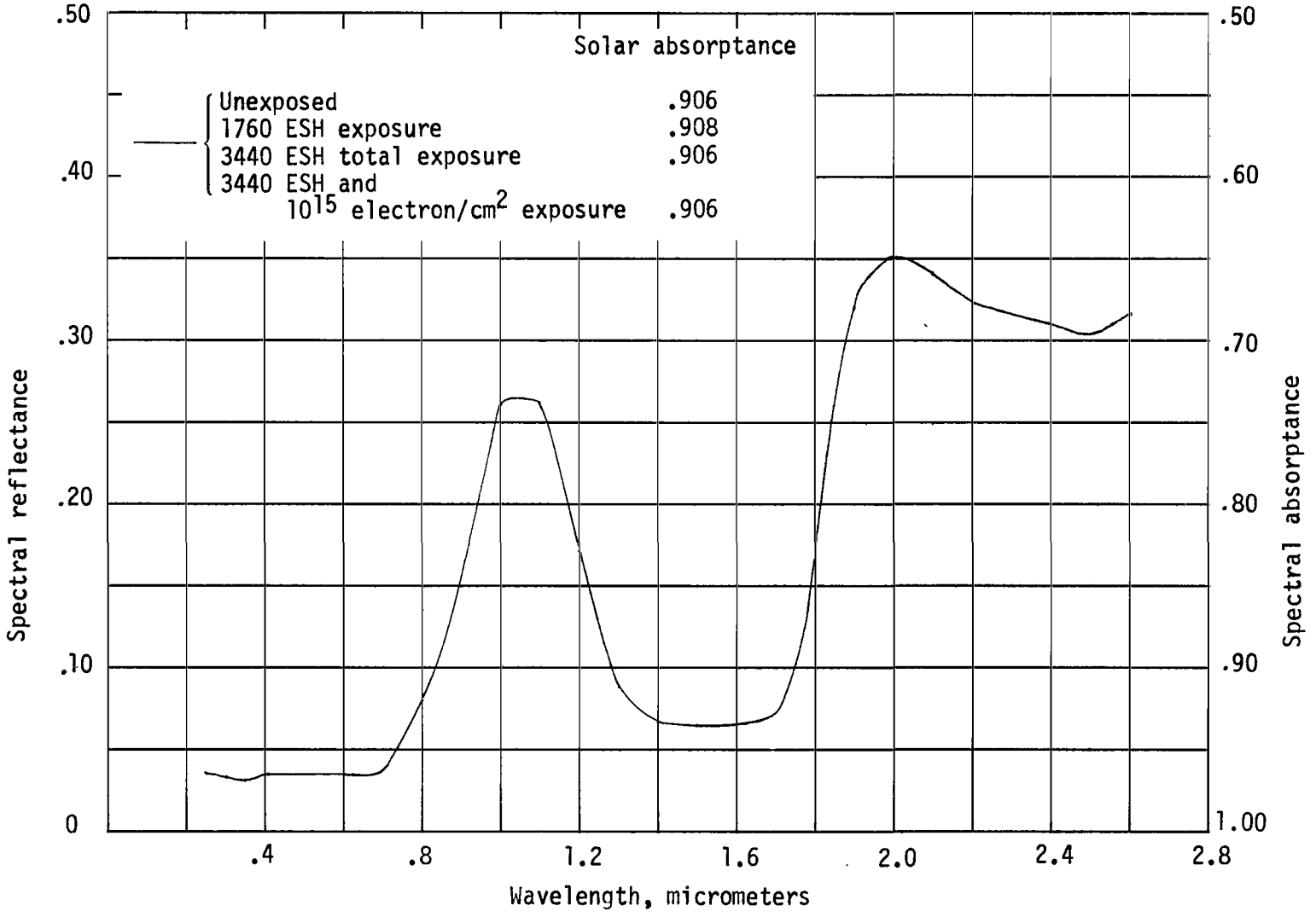

(n) Pyromark Black on inconel.

Figure 4.- Continued.

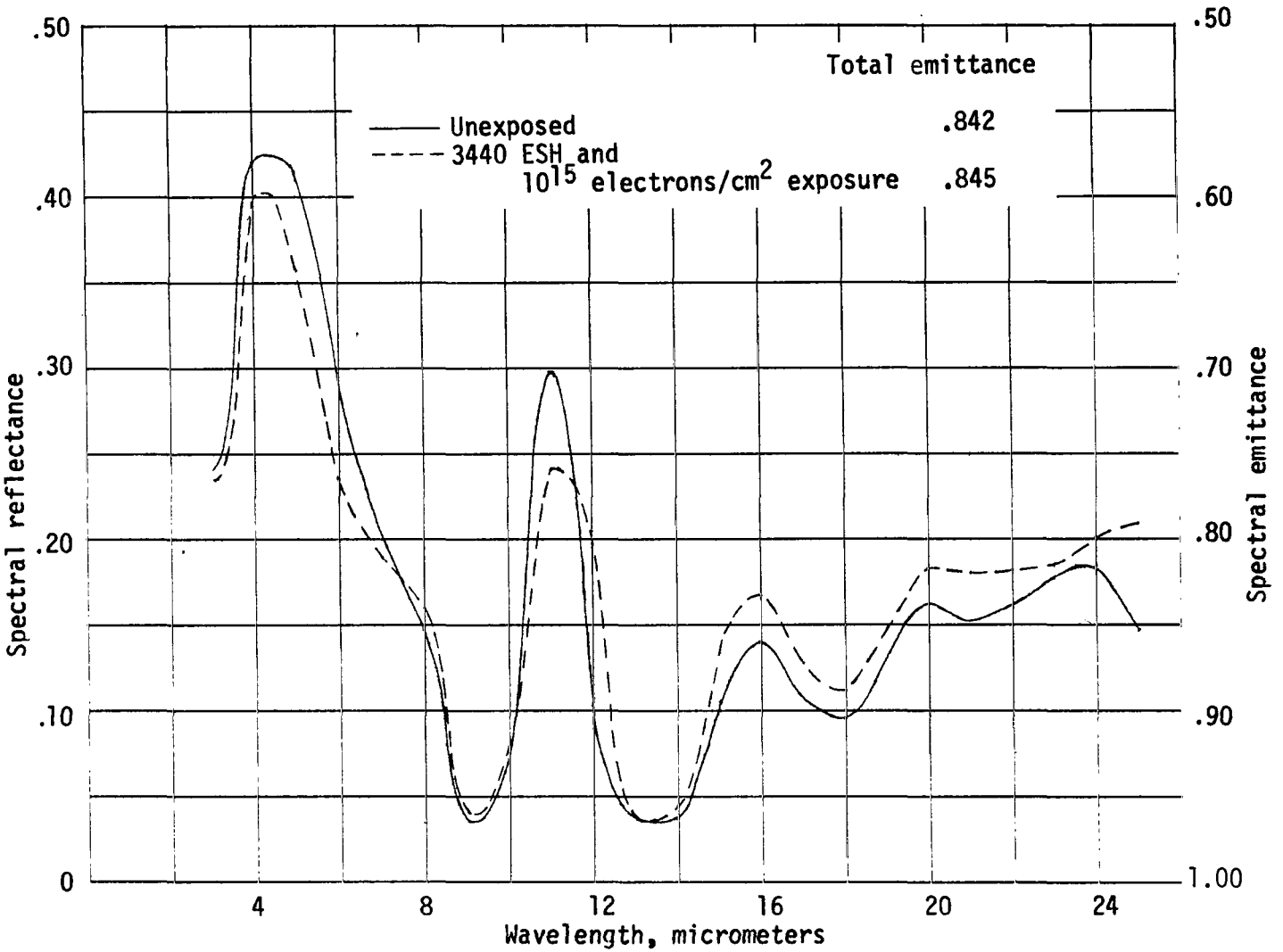

(n) Concluded.

Figure 4.- Concluded.

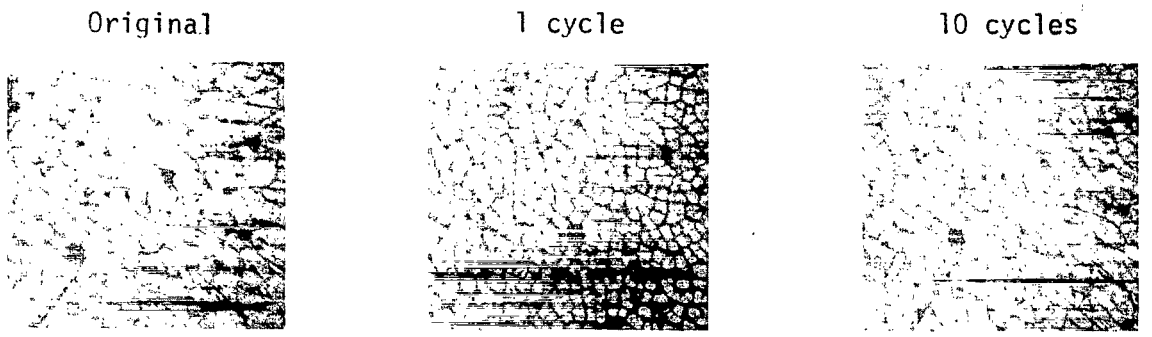

(a) NiS dyed anodized aluminum sample showing crazing also typical of CoS dyed anodized aluminum.

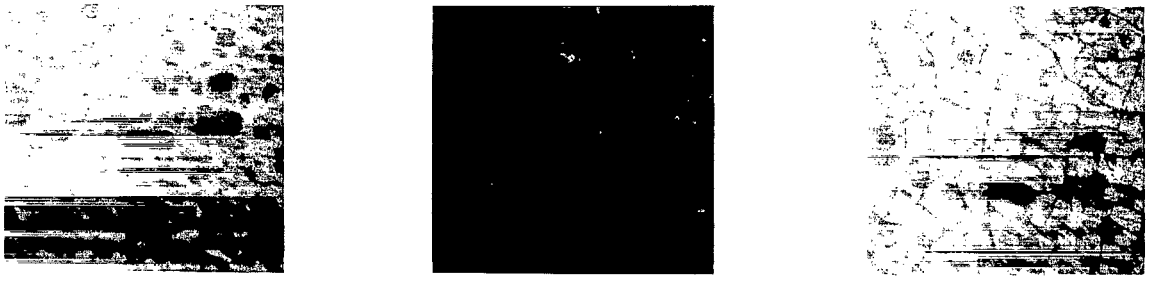

(b) PbS dyed anodized aluminum sample showing crazing also typical of Sandoz black BK, Sandoz black OA, and Bi_2S_3 dyed anodized aluminum.

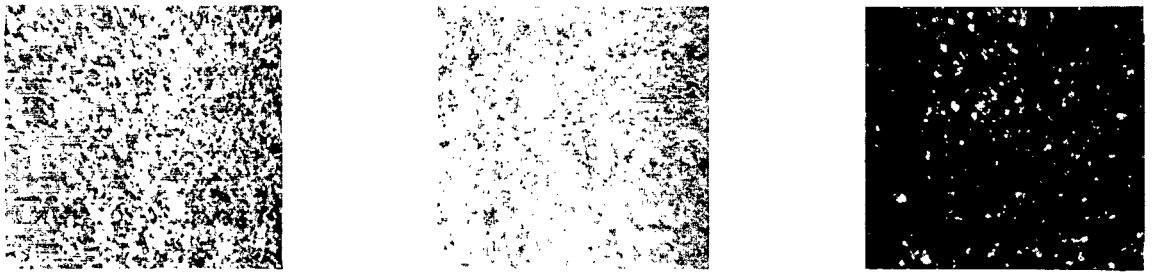

(c) Black nickel plate on aluminum showing no effects; also typical Pyromark Black, Du-Lite 3-0, and sodium dichromate blackened samples.

L-67-973

Figure 5.- Photomicrographs illustrating effects of thermal shock on various coated test samples. Magnification, X 70.

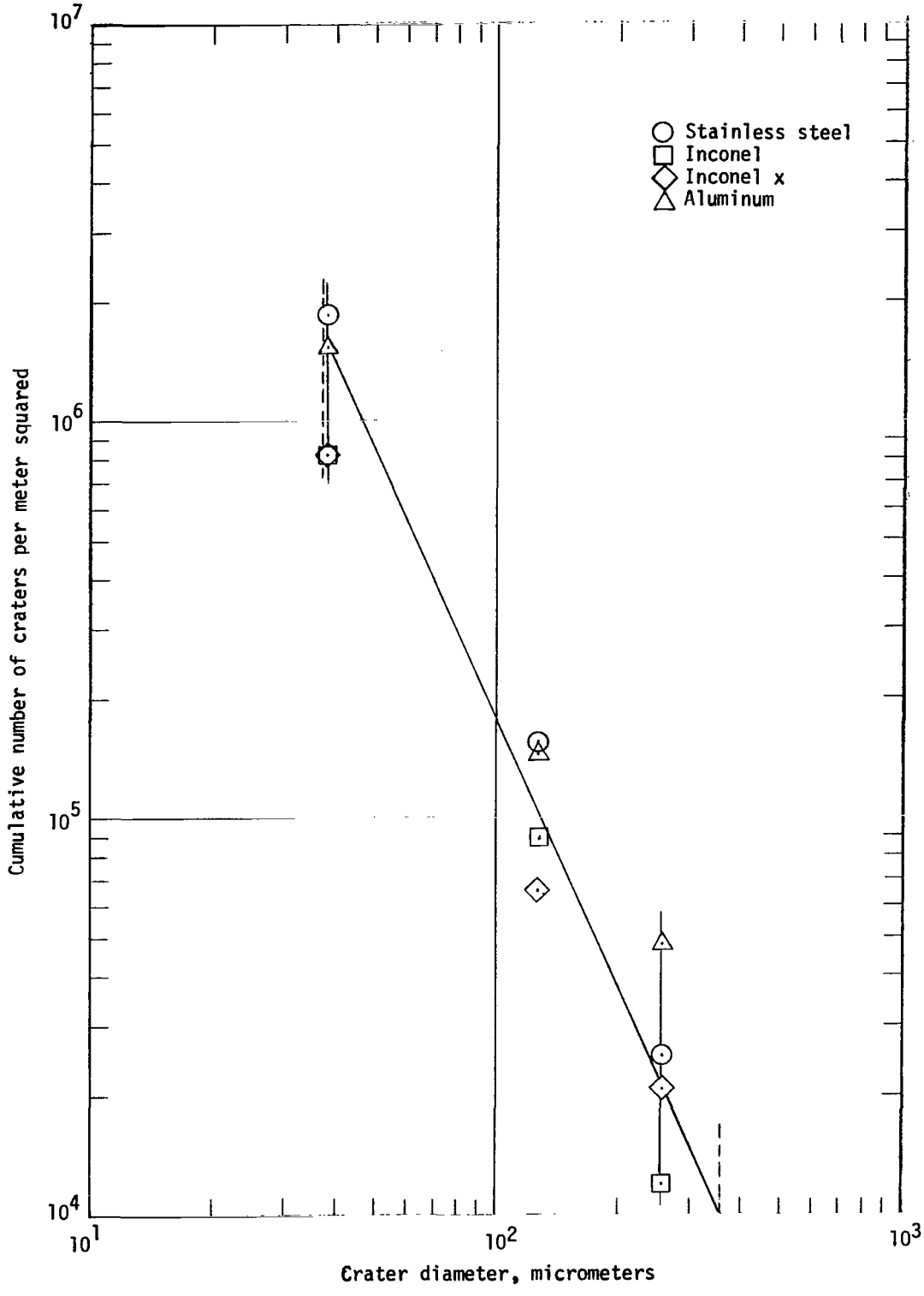

Figure 6.- Cumulative number of craters formed by shaped charges on calibration plates on the basis of crater size for various materials.

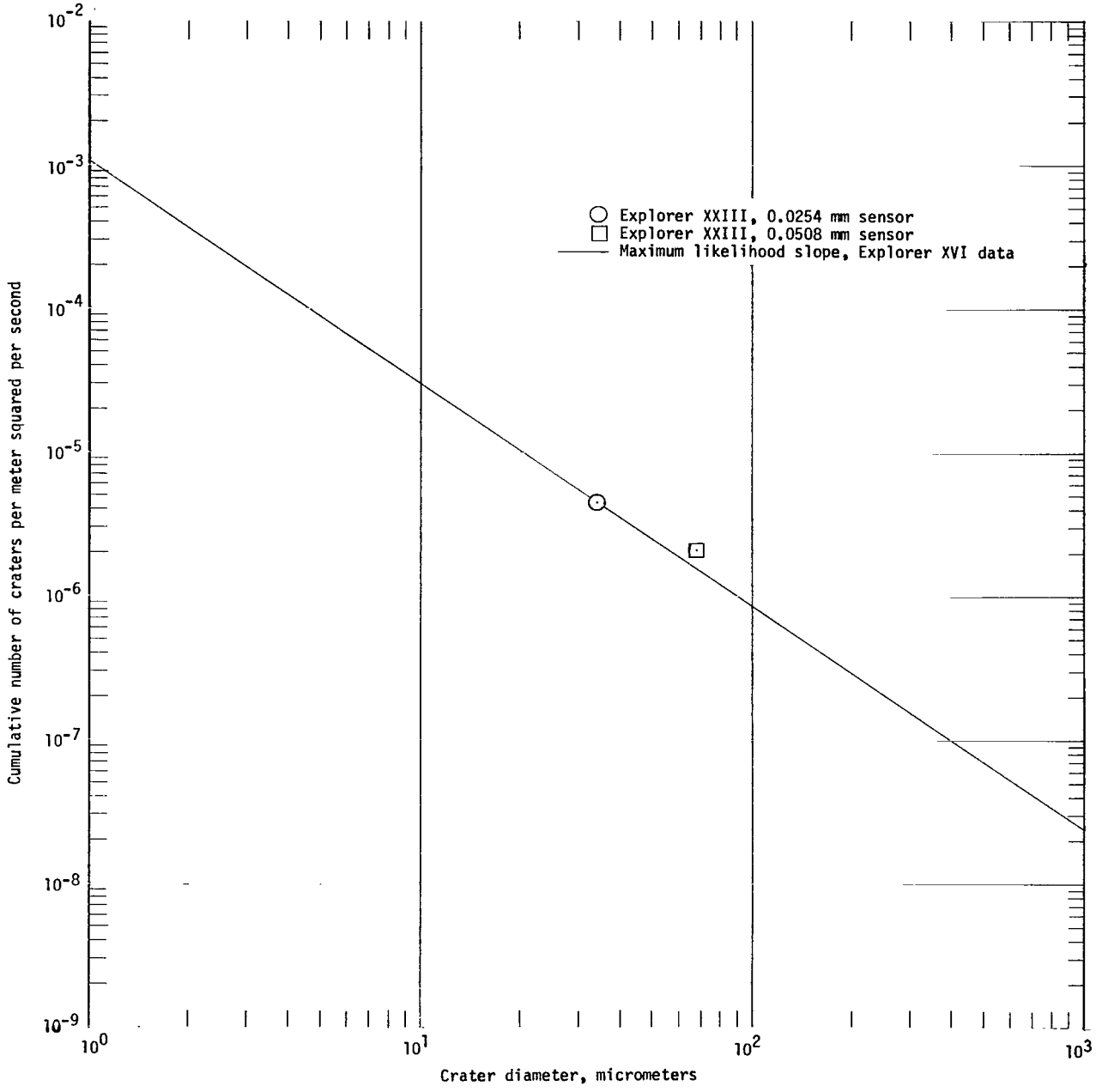

(a) Stainless steels.

Figure 7.- Cumulative number of craters compared with crater size.

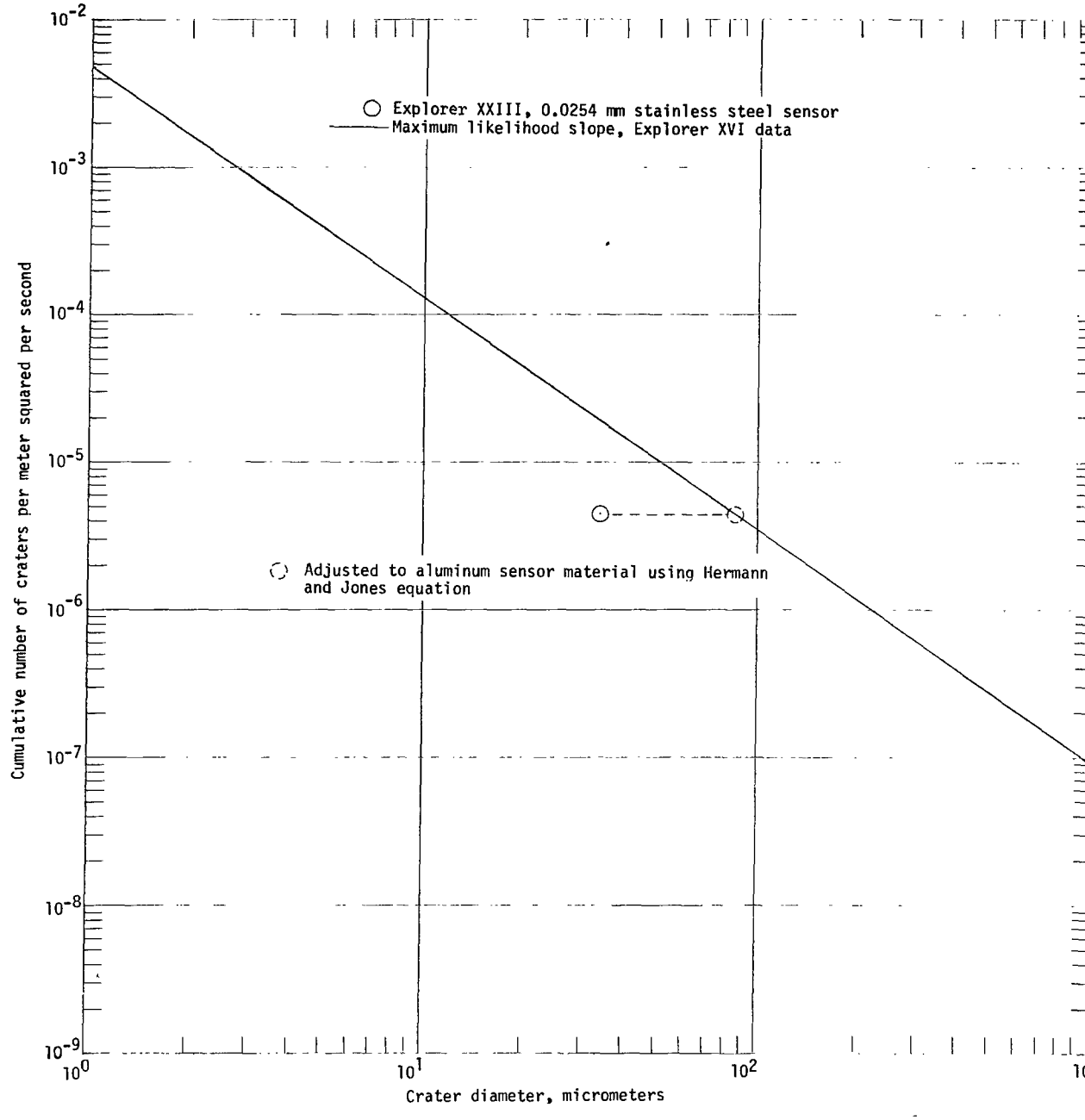

(b) 1100 (2-S) aluminum.

Figure 7.- Concluded.

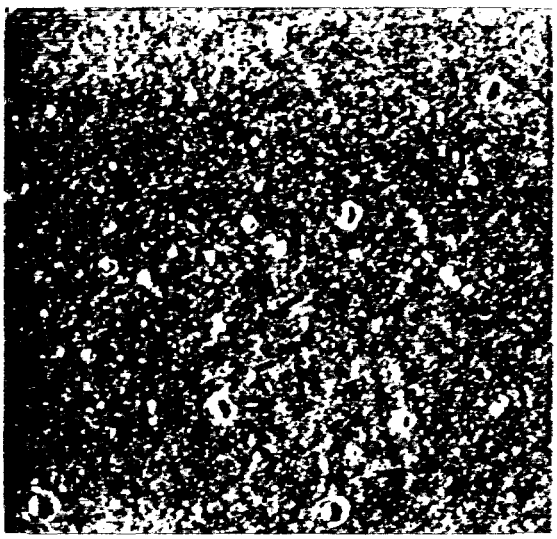

(a) Pyromark Black on inconel. Coating ≈ 32 μm.

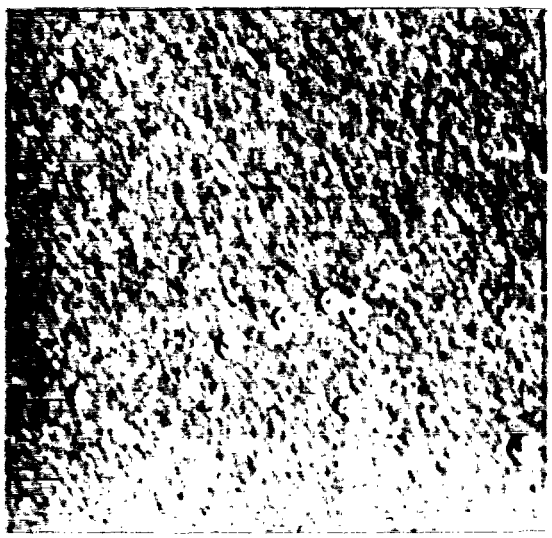

(b) Pyromark Black on 1100 (2-S) aluminum. Coating ≈ 32 μm.

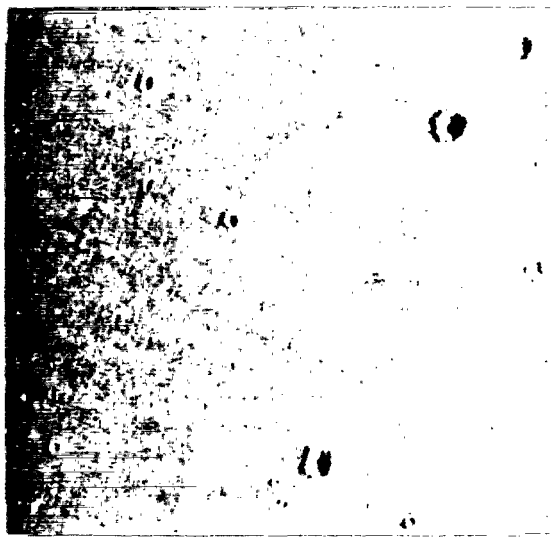

(c) Du-Lite 3-0 on grit blasted type 304 stainless steel. Coating ≈ 3 μm.

(d) Black nickel plate on 1100 (2-S) aluminum. Coating ≈ 3 μm.

L-67-974

Figure 8.- Photomicrographs illustrating the effect of micrometeoroid impact on thick coatings (≈32 μm) and thin coatings (≈3 μm). (Area shown is 1 cm^2 magnified X 8.)

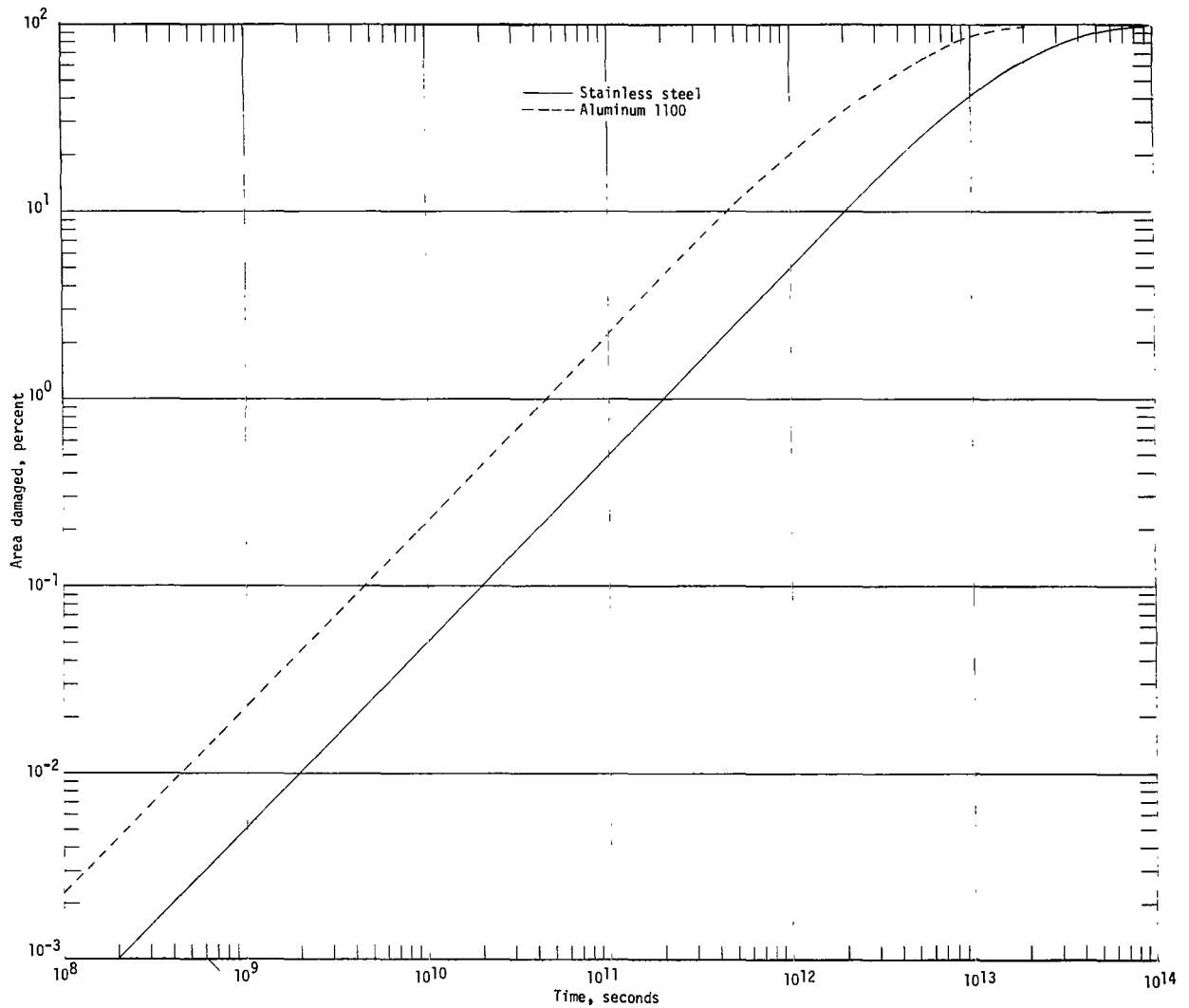

Figure 9.- Variation of percent of area damaged by micrometeoroids with time for stainless steel and aluminum as calculated from Explorer XVI and XXIII micrometeoroid penetration data.

"The aeronautical and space activities of the United States shall be conducted so as to contribute . . . to the expansion of human knowledge of phenomena in the atmosphere and space. The Administration shall provide for the widest practicable and appropriate dissemination of information concerning its activities and the results thereof."

—NATIONAL AERONAUTICS AND SPACE ACT OF 1958

NASA SCIENTIFIC AND TECHNICAL PUBLICATIONS

TECHNICAL REPORTS: Scientific and technical information considered important, complete, and a lasting contribution to existing knowledge.

TECHNICAL NOTES: Information less broad in scope but nevertheless of importance as a contribution to existing knowledge.

TECHNICAL MEMORANDUMS: Information receiving limited distribution because of preliminary data, security classification, or other reasons.

CONTRACTOR REPORTS: Scientific and technical information generated under a NASA contract or grant and considered an important contribution to existing knowledge.

TECHNICAL TRANSLATIONS: Information published in a foreign language considered to merit NASA distribution in English.

SPECIAL PUBLICATIONS: Information derived from or of value to NASA activities. Publications include conference proceedings, monographs, data compilations, handbooks, sourcebooks, and special bibliographies.

TECHNOLOGY UTILIZATION PUBLICATIONS: Information on technology used by NASA that may be of particular interest in commercial and other non-aerospace applications. Publications include Tech Briefs, Technology Utilization Reports and Notes, and Technology Surveys.

Details on the availability of these publications may be obtained from:

SCIENTIFIC AND TECHNICAL INFORMATION DIVISION

NATIONAL AERONAUTICS AND SPACE ADMINISTRATION

Washington, D.C. 20546